AMRL-TDR-63-18

SOME DYNAMIC RESPONSE CHARACTERISTICS OF WEIGHTLESS MAN

Charles Edward Whitsett, Jr., Captain, USAF

TECHNICAL DOCUMENTARY REPORT NO. AMRL-TDR-63-18

April 1963

Behavioral Sciences Laboratory
6570th Aerospace Medical Research Laboratories
Aerospace Medical Division
Air Force Systems Command
Wright-Patterson Air Force Base, Ohio

Project No. 7184, Task No. 718405

NOTICES

When US Government drawings, specifications, or other data are used for any purpose other than a definitely related government procurement operation, the government thereby incurs no responsibility nor any obligation whatsoever; and the fact that the government may have formulated, furnished, or in any way supplied the said drawings, specifications, or other data is not to be regarded by implication or otherwise, as in any manner licensing the holder or any other person or corporation, or conveying any rights or permission to manufacture, use, or sell any patented invention that may in any way be related thereto.

Qualified requesters may obtain copies from the Defense Documentation Center for Scientific and Technical Information (DDC), Arlington Hall Station, Arlington 12, Virginia. Orders will be expedited if placed through the librarian or other person designated to request documents from DDC (formerly ASTIA).

Do not return this copy. Retain or destroy.

Stock quantities available at Office of Technical Services, Department of Commerce, Washington 25, D. C. Price per copy is $1.50.

Change of Address

Organizations receiving reports via the 6570th Aerospace Medical Research Laboratories automatic mailing lists should submit the addressograph plate stamp on the report envelope or refer to the code number when corresponding about change of address.

37-914, 900, 7-31-63

FOREWORD

This report was prepared by Captain Whitsett in partial fulfillment of the requirements for the Master of Science Degree in Engineering at the USAF Institute of Technology in 1962. The topic was selected from a list of requirements under the Behavioral Sciences Laboratory Project No. 7184, "Human Performance in Advanced Systems," Task No. 718405, "Design Criteria for Crew Stations in Advanced Systems."

Special acknowledgment is made to Captain Simons of the Crew Stations Branch, Human Engineering Division, Behavioral Sciences Laboratory, 6570th Aerospace Medical Research Laboratories, and Lieutenant Bucciarelli, thesis adviser, for their sincere interest, suggestions, and guidance throughout this study. Also, thanks are extended to T/Sgt Harold Espensen and M/Sgt C.W. Sears of the Crew Stations Branch for conducting the zero-gravity experiments and for serving as subjects, and to Mr. Charles E. Clauser, Anthropology Branch, Human Engineering Division, for his suggestions on the mathematical model.

ABSTRACT

By segmenting the body into 14 idealized masses, a mathematical model is developed to approximate the mass distribution, center of mass, moments of inertia, and degrees of freedom of a human being. An analysis of the model reveals that the segment moments of inertia about the mass centers of the hands, feet, and forearms are negligible when compared to the total body moments of inertia, although the torso moment of inertia is not negligible. Some selected problems in thrust misalignment, free-body dynamics, stability of rotation, and torque application are solved analytically to predict man's dynamic response characteristics in space. Preliminary experiments indicate that the torque which weightless man can exert by applying a sudden twist to a fixed handle varies as a half-sine wave, and is approximately 67% of his maximum torque under normal gravity conditions.

PUBLICATION REVIEW

This technical documentary report has been reviewed and approved.

Walter F. Grether

WALTER F. GRETHER
Technical Director
Behavioral Sciences Laboratory

TABLE OF CONTENTS

LIST OF ILLUSTRATIONS

LIST OF TABLES

LIST OF SYMBOLS

A	a constant
a	semi-major axis of ellipse
a′	acceleration
B	a constant
b	semi-minor axis of ellipse
C	constant of integration
c	instep length of foot
D	distance
d	diameter
$\hat{E}$	unit vector corresponding to the (X′, Y′, Z′) Body Fixed Axis System at the mass center of mass m_1
$\hat{e}$	unit vector corresponding to the (X, Y, Z) Body Fixed Axis System at the mass center of mass m_2
F	thrust force
H	resultant angular momentum
h	angular momentum of an individual mass
I	moment of inertia
i	a typical mass
$\hat{i}$	unit vector in the Body Axis System
$\hat{i}'$	unit vector in the Inertial System
$\hat{j}$	unit vector in the Body Axis System
$\hat{j}'$	unit vector in the Inertial System
K	a number representing $\epsilon F/2I_Y$
$\hat{k}$	unit vector in the Body Axis System
$\hat{k}'$	unit vector in the Inertial System
ℓ	length
M	moment or torque
m	mass of segment

LIST OF SYMBOLS (Continued)

N	a number representing $2I_v/\epsilon m$
n	number of segments which change position from the initial condition
P	total number of masses
Q	magnitude of position vector from the hinge point to the individual mass center
R	largest radius of the frustum
r	smallest radius of the frustum
T	total period
$\dot{T}$	kinetic energy
t	time
V	velocity
X_n	nondimensional number representing $\frac{mK}{F} X_o$
X	Body Axis System coordinate
X′	Inertial System coordinate
Y	Body Axis System coordinate
Y′	Inertial System coordinate
Z_n	nondimensional number representing $\frac{mK}{F} Z_o$
Z	Body Axis System coordinate
Z′	Inertial System coordinate
c.m.	mass center of each mass
c.c.m.	mass center of entire system
α	angle between spin axis and angular momentum vector
β	angle between Z and Z'
γ	smallest angle between Q_1 and Q_2
Δ	D_1 minus D_2, by definition
δ	average density
ϵ	magnitude of position vector
η	ratio of $\hat{Y}/\ell$

LIST OF SYMBOLS (Continued)

θ	angle through which the torso is tilted backward
λ	net angular velocity of system
μ	ratio of r/R
ν	an integral by definition $\int \Omega\,(t)dt$
ρ	radius of curvature
σ	a nondimensional number representing $1 + \mu + \mu^2$
τ	a time parameter representing $(Kt^2)^{\frac{1}{2}}$
Φ	swing angle of arms
Ψ	nondimensional ratio of masses, $\frac{m_2}{m_1}$
Ω	angular velocity of mass, m_1
ω	angular velocity

LIST OF SUBSCRIPTS

$_o$	at the initial condition
$_c$	resultant about the mass center
$_{cg}$	about the center of gravity
$_i$	a typical mass
$_M$	maximum
$_n$	nondimensional
$_{tot}$	total
$_x$	about the X-axis
$_y$	about the Y-axis
$_z$	about the Z-axis

$_{xy}$, $_{yz}$, and $_{zx}$ are planes for the products of inertia

SOME DYNAMIC RESPONSE CHARACTERISTICS OF WEIGHTLESS MAN

INTRODUCTION

The purpose of this study is to develop a mathematical model to represent the human body, and to use this model to predict man's mechanical behavior in some selected conditions associated with weightlessness. The problems of dynamics facing the weightless man are many and varied. As Simons and Kama (ref. 19) stated: "Free-floating man is indeed an intimate man-machine unit, a single vehicle-driver component capable of fantastic motion behavior."

As space operations are extended, man will be required to perform supply, assembly, maintenance, and rescue missions while weightless. Man in space, floating free from his space vehicle, will experience degrees of freedom never encountered on earth. While "situated in a state of imponderability" (as Petrov has described weightlessness, ref. 15), any force applied to or by man will result in translational and/or angular accelerations. For instance, the force of an ordinary sneeze is sufficient to tumble the average unrestrained individual at a rate of one-fifth of a revolution per minute (ref. 21).

If the free-floating space worker is to move from one point to another and be able to work when he gets there, he must be provided with a personal propulsion and stabilization device (refs. 9, 17, and 18). Before such a system can be developed, however, certain design parameters must be established. These parameters are dependent upon the biomechanical properties of the human body. To bridge the gap between anthropometric data and the dynamic response characteristics needed for engineering design, a mathematical model is constructed. "Dynamic response characteristics" is used here to describe those mechanical effects which result when the human body is subjected to unbalanced forces.

Many of the biomechanical properties of the body change when its shape changes. For instance, when man moves his arms or legs, his center of mass and moments of inertia change. Since the human body is complex and flexible, any convenient analytical representation is only an approximation. As two bio-engineers (ref. 3) have so aptly put it, man is a "non-symmetrical, fluid-filled sack of variable shape containing a large air bubble."

Scope

This study is concerned with only those major dynamic effects which result when the human body is subjected to unbalanced forces, and not the resulting physiological and psychological effects.

A general survey is made of some selected free-body dynamics problems in which the kinematics of the body are simple, and where elasticity and damping of the body structure are neglected.

The experimental efforts are preliminary and may serve as guidelines for future study.

Development

The problem of describing or predicting the dynamic response characteristics of weightless man is approached in three phases:

a. Description and analysis of a mathematical model

b. Analytical prediction of some selected dynamic response characteristics

c. Comparison of some analytical results with experimental data

The first phase of this study is devoted to the development of a mathematical model which incorporates the biomechanical and anthropometric properties of man. Using a model based on 50th percentile data of the 1950 USAF population (ref. 12), an analysis is made to determine the contribution of each of the various body moments of inertia. This model will herein be called the USAF Mean Man. Based on this analysis, a simplified method is developed for calculating the changes in moments of inertia and center of mass when the body posture changes.

In the second phase some selected dynamics problems are investigated which can be used to analytically predict some of the dynamic response characteristics of weightless man.

The third phase covers the results of the experimental validation phase of the study.

THE MATHEMATICAL MODEL

Weightless man will undergo transient angular and linear accelerations and decelerations as he is subjected to unbalanced external forces. Internal forces and/or moments will be generated and will react throughout the body when he moves his appendages. The mechanical response of the human body to these forces will depend upon its biomechanical properties. To develop a mathematical model which can be used to predict how the human body will respond, these same biomechanical properties must be incorporated into the model.

The human body is a complex system of elastic masses whose relative positions change as the appendages are moved. To represent this system in exact analytical terms would require an infinite number of infinitesimal, rigid masses and an infinite number of degrees of freedom. "Degrees of freedom" refers to the minimum number of independent coordinates necessary to completely specify the position of a system in space. As larger and fewer masses are chosen, the representation becomes less complex but also less accurate. The problem reduces to a determination of the optimum number and shapes of the idealized body segments on which to base dynamic response characteristics. The criteria for development of the model are:

a. Simplicity - the minimum number of components of simple geometrical shape consistent with an accurate representation of the human body

b. Adaptability - the ability of the model to incorporate the biomechanical properties of any particular individual

A simple, but reasonably accurate, model is desired to simplify analytical solutions to the related dynamics problems and make it easier to interpret the results. The degree of accuracy required depends upon the particular problem being investigated. For instance, when the flight characteristics of a fighter aircraft are computed, the pilot is assumed to be a point mass at some location in the fuselage. In this case the dynamic characteristics of the man are negligible when compared to those of the aircraft. However, when individual propulsion and stabilization devices for a space worker are considered, man's dynamic response characteristics become very important. In this case, dynamic characteristics of the whole system depend primarily on the man since his size and mass may equal or surpass that of the propulsion and stabilization unit. Since a model for the latter application is desired for this study, a more refined model is developed than has been previously described (refs. 14, 18).

Since the propulsion and stabilization unit may be tailored to each space worker, the mathematical model must be able to accommodate any individual.

Development of the Model

The most important biomechanical properties which will affect the dynamic response characteristics of man, and hence must be incorporated in the model, are:

a. Mass and mass distribution

b. Location of the center of mass

c. Moments of inertia

d. Elasticity and damping of the body structure

Items b and c vary as the body position changes. This variation will affect man's response characteristics. Item d becomes significant only when forces are applied very suddenly such as during an impact; hence, it is not included in this study.

To develop the mathematical model, the following assumptions are made:

a. The human body consists of a finite number of masses (or segments) and a finite number of degrees of freedom (hinge points).

b. The segments are rigid and homogeneous.

c. Each segment is represented by a geometric body which closely approximates the size, shape, mass, and center of mass of the segment.

The dynamic properties of these rigid, homogeneous, geometric bodies can be exactly determined.

Configuration of the Model:

The mathematical model may be thought of as a system of rigid, homogeneous bodies of relatively simple geometric shape, hinged together to resemble the human body. For this study a 14-segment model is chosen. The division of the body into segments and the representative geometric bodies are shown in figure 1.

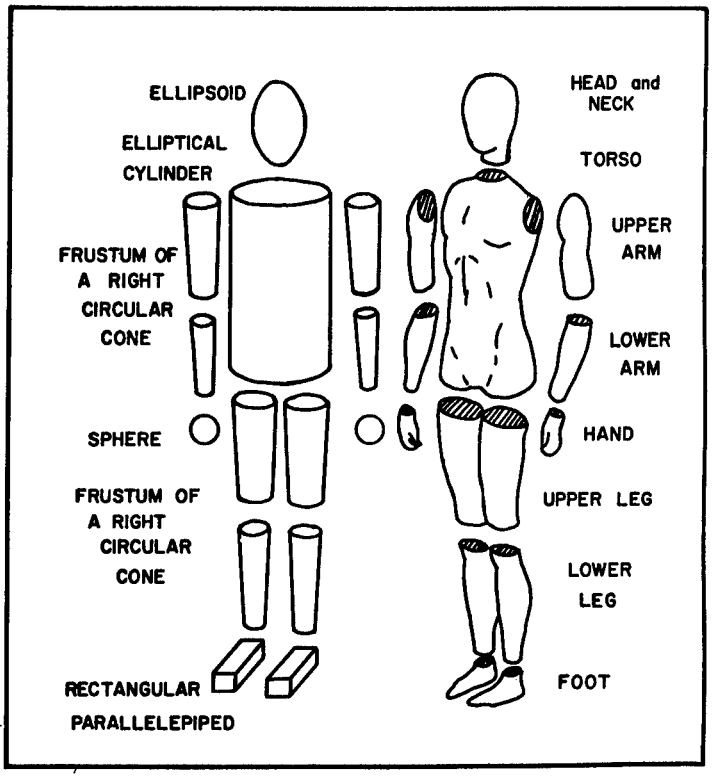

Figure 1. Segmented Man and Model

The hinge points are shown in figure 2 and are defined as:

a. Neck - hinged only at the base of the neck

b. Shoulder - hinged at the arm-shoulder socket

c. Elbow - hinged at the elbow joint

d. Hip - hinged at the leg-pelvis socket

e. Knee - hinged at the knee joint

The ankle and wrist joints are assumed to be rigid, since their motion produces very slight variations in the total center of mass and moments of inertia.

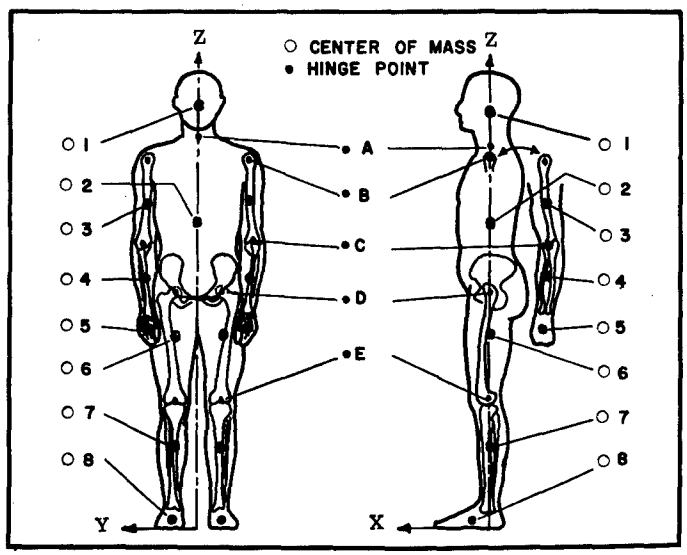

Figure 2. Location of Centers of Mass and Hinge Points of the Human Body

The model described has 24 degrees of freedom—6 rigid body degrees of freedom plus 18 local degrees of freedom. The six rigid body degrees of freedom refer to the position and orientation of the body axis system. The other 18 degrees of freedom result from the 9 hinge points, each with 2 degrees of freedom. For instance, if a set of spherical coordinates is located at one shoulder-hinge point, two angles must be specified to exactly locate the position of the upper arm.

The body axis system, shown in figure 3, consists of a set of three orthogonal axes whose origin is always at the body center of mass and whose orientation remains fixed with respect to the axis system of the elliptical cylinder, as shown in figure 4. The Z-axis remains parallel to the cylindrical axis, the X-axis perpendicular to the major and cylindrical axes, and the Y-axis perpendicular to the minor and cylindrical axes. The positive directions and rotations are indicated in figure 3.

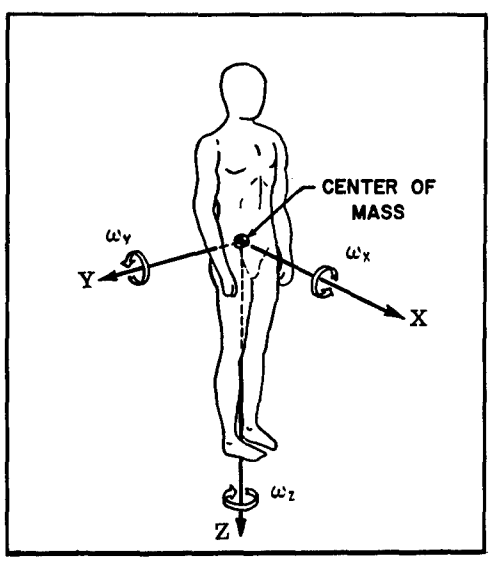

Figure 3. Body Axis System

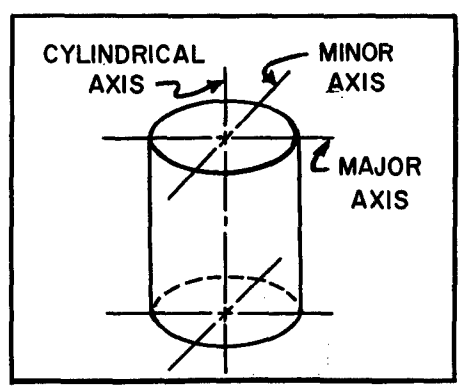

Figure 4. Elliptical Cylinder

A local body axis system is defined as a secondary orthogonal axis system located at the center of mass of each segment. Each local body axis system is initially oriented in the same direction as the primary body axis system, the position defined in figure 3. However, as the segment moves, the local system remains fixed in position and direction with respect to that segment.

Biomechanical Properties:

For the model to represent the dynamic response characteristics of man, certain biomechanical properties must be incorporated into the model. As stated earlier, these properties include mass, center of mass, average density, body dimensions, and moments of inertia. When these properties are used to define the characteristics of the geometric bodies which make up the model, the model will reflect the dynamic response characteristics of man. Some problems arise when the model is to represent a particular individual, since methods have not been developed for determining all these properties from living subjects. Fortunately, body dimension can be readily attained. Hence, for the model developed, only body measurement data (lengths of the segments, depths, breadths, and hinge point locations) is taken from the living subject. All other properties are estimated by the most reliable statistical methods available for various weight and body build groups. The methodology of obtaining the biomechanical properties of all the segments is described below.

The masses of all segments, except the head and torso, are estimated from the regression equations given by Barter (ref. 1) and are summarized in table I. The head and torso equations are not given separately. Therefore, a method of determining the mass of these segments is developed.

TABLE I

REGRESSION EQUATIONS FOR COMPUTING THE MASS OF BODY SEGMENTS (ref. 1, p. 6)
(in kg)

Body Segment	Regression Equation
Both Upper Arms	0.08 × Total Body Weight - 1.3
Both Lower Arms	0.04 × Total Body Weight - 0.2
Both Hands	0.01 × Total Body Weight + 0.3
Both Upper Legs	0.18 × Total Body Weight + 1.5
Both Lower Legs	0.11 × Total Body Weight - 0.9
Both Feet	0.02 × Total Body Weight + 0.7

The center of mass location for the upper and lower arms and legs is taken directly from Dempster (ref. 4), and is given later in table V. For the other segments the center of mass is at one-half the length and on the axis of symmetry. The average density for all segments is also based on Dempster's study, and listed in table V.

The lengths of the segments (defined as the vertical dimension of each segment as oriented in figure 1) are based on the body measurement data determined as indicated in table II. The points and methods of measuring are given in ref. 12. Alternatively, the lengths may be taken directly from ref. 12 for a particular percentile group.

TABLE II

SEGMENT LENGTH FROM ANTHROPOMETRY

Segment	Length
Head	Stature - Cervical Height
Torso	Cervical Height - Penale Height
Upper Arm	Shoulder Height - Elbow Height
Lower Arm	Elbow Height - Wrist Height
Upper Leg	Penale Height - Kneecap Height +1.5 inches
Lower Leg	Kneecap Height - Lateral Malleolus Height -1.5 inches
Foot	Lateral Malleolus Height

NOTE: All heights are defined in ref. 12

The equations for calculating the mass moments of inertia for all the geometric bodies used in the model, except the frustum, are found in most mechanics textbooks (for example, ref. 5) and engineering handbooks (such as ref. 13). The equations for the mass moments of inertia of a frustum of a right circular cone are developed, in parametric form based on the center of mass location, in Appendix A. All equations are summarized in table III.

TABLE III

FORMULAS FOR CALCULATING LOCAL MOMENTS OF INERTIA OF THE SEGMENTS

	Moments of Inertia		
Segment	$I_{x_{cg}}$	$I_{y_{cg}}$	$I_{z_{cg}}$
Head	$\frac{1}{5} m(a^2 + b^2)$	$I_{x_{cg}}$	$\frac{2}{5} m a^2$
Torso	$\frac{1}{12} m(3a^2 + \ell^2)$	$\frac{1}{12} m(3b^2 + \ell^2)$	$\frac{1}{4} m(a^2 + b^2)$
Upper and Lower Arms and Legs	$m\left[A\left(\frac{m}{\delta \ell}\right) + B\ell^2\right]$	$I_{x_{cg}}$	$2\frac{m^2}{\delta \ell} A$
Hand	$\frac{2}{5} m \left(\frac{d}{2}\right)^2$	$I_{x_{cg}}$	$I_{x_{cg}}$
Foot	$\frac{1}{6} m \ell^2$	$\frac{1}{12} m(c^2 + \ell^2)$	$I_{y_{cg}}$

The other basic dimensions required for the moment of inertia equations (such as the diameter, major axis, and minor axis) depend upon the particular segment. Their determination is included with the following general discussion of the geometric bodies chosen to represent each particular segment of the human body.

Head, Hand, and Foot. —The motion of the neck is small in comparison to that of the head. Hence, the neck is considered to be rigidly attached to the head. The head-neck combination is then represented by an ellipsoid of revolution. The major axis, 2a, is equal to the length dimension given in table II. The minor axis, 2b, is found from:

$$2b = \frac{\text{head circumference}}{\pi} \tag{1}$$

since the cross-section is circular.

The mass, m, is given by:

$$m = \frac{4}{3} \delta \pi a b^2 \tag{2}$$

where δ is the average density of the head.

The mass of the hand is very small in comparison to the whole body (about 0.7%) and, even though its shape varies considerably, the effect of this variation is negligible. Hence, the hand is greatly simplified and represented by a sphere. From:

$$m = \frac{4}{3} \delta \pi \left(\frac{d^3}{8}\right) \tag{3}$$

we have:

$$\text{diameter } d = 2\left(\frac{3m}{4\delta\pi}\right)^{\frac{1}{3}} \tag{4}$$

The mass of the foot is quite small in comparison to the whole body (about 1.5%); hence, it too is greatly simplified. The foot is represented by a rectangular parallelepiped whose height and width equals the length dimension for the foot given in table II. The depth is equal to the instep length, c (ref. 12).

Torso. —The torso makes up approximately 48.5% of the total body mass. Consequently, its biomechanical properties will have a significant effect on the total body response.

An elliptical cylinder is chosen to represent the torso. The dimensions of the ellipse of the cross-section are given by:

Major axis (a) - Equal to the average of the body breadth measured at the chest, waist, and hips

Minor axis (b) - Equal to the average of the body depth measured at the chest, waist, and hips

To further substantiate the choice of an elliptical cylinder to represent the torso, a more detailed study was made to compare the average cross-sectional area of the human body to that of an ellipse based on the average breadth and depth.

Full-scale, cross-sectional area projections of the torso of a living subject of average build were provided by the Anthropology Branch of the Behavioral Sciences Laboratory. These were obtained by stereophotogrammetry (a photographic method of making contour maps of the human body). The cross-sectional areas at the chest, waist, and hip were measured with a planimeter. The average area of the subject was 107.7 square inches. The breadth and depth were measured at the corresponding levels and averaged. The area of the representative ellipse was found to be 106.0 square inches from:

$$\text{Area of ellipse} = \pi ab \tag{5}$$

where:

$$a = \tfrac{1}{2} \text{ average breadth} \tag{6}$$

$$b = \tfrac{1}{2} \text{ average depth} \tag{7}$$

Of course, the comparison for just one subject does not in itself justify the assumption that the torso can be represented by an elliptical cylinder. It does indicate that this is a reasonable approach.

Limbs. —A frustum of a right circular cone is chosen to represent the upper and lower arms and legs because its center of mass can be made to coincide with that of the segment it represents. Parametric equations for moments of inertia are developed in Appendix A which are independent of all segment dimensions except length (given in table II). A sample calculation is also given in Appendix A which illustrates the use of the parametric equations. Since there is no published USAF anthropometric data which coincides well with the height of the knee joint, this dimension is estimated by subtracting 1.5 inches* from the kneecap height.

Hinge Points. —The hinge points are assumed to be on the center line of the segments and are defined in table IV.

TABLE IV

LOCATION OF HINGE POINTS FROM ANTHROPOMETRY

Hinge Point	Coordinates†	
	Y	Z
Neck	0	Cervical Height
Shoulder	$\pm \frac{1}{2}$ Biacromial Diameter	Shoulder Height
Elbow	$\pm \frac{1}{2}$ Biacromial Diameter	Elbow Height
Hip	$\pm \frac{1}{4}$ Hip Breadth	Penale Height
Knee	$\pm \frac{1}{4}$ Hip Breadth	Kneecap Height - 1.5 inches

†All X-coordinates are zero

NOTE: All measurements are defined in ref. 12

Analysis of the Model

Since the center of mass and moments of inertia depend upon the positions of the body segments, an analysis based on only one position is likely to lead to some false conclusions. This section presents an analysis of the proposed mathematical model in two quite different positions.

---

* *This estimation is based on unpublished data by Charles E. Clauser, Anthropology Branch, Human Engineering Division, Behavioral Sciences Laboratory.*

Numerical Values:

Numerical values of the biomechanical properties of the model are determined for the USAF mean man (height 69.11 inches, weight 163.66 pounds) as described in Anthropometry of Flying Personnel-1950 (ref. 12). The weight, average density, length, and center of mass location of each segment are given in table V. From this data the coordinates of the hinge points and segment centers of mass, as defined in figure 2, are determined and presented in table VI. Note that the origin of the coordinate system in figure 2 is shifted to floor level. The coordinates in table VI are given in terms of this transposed coordinate system since all heights in ref. 12 are based on distance from the floor. From the data in tables V and VI and the formulas in table III, the local moments of inertia are calculated and given in table VII. The moments of inertia of each segment about the body axes are found from the parallel axis transfer equation:

$$I = I_{cg} + mD^2 \tag{8}$$

where I_{cg} is the local moment of inertia, m is the mass of the segment, and D is the distance between the body axis and a parallel axis through the center of mass of the segment. These values are also given in table VII.

TABLE V

BIOMECHANICAL PROPERTIES OF THE SEGMENTS OF THE USAF MEAN MAN

Segment	Weight (lbs)	Density (lbs/ft^3)	Length (inches)	Centroid Location (% length)
Head	11.20	71.6	10.04*	50.0
Torso	78.90	68.6	24.56*	50.0
Upper Arm	5.10‡	70.0	13.00*	43.6†
Lower Arm	3.03‡	70.0	10.00*	43.0†
Hand	1.16‡	71.7	3.69	50.0
Upper Leg	16.33‡	68.6	15.80*	43.3†
Lower Leg	8.05‡	68.6	15.99*	43.3†
Foot	2.39‡	68.6	2.73*	50.0

*Ref. 12

†Ref. 4

‡Mr. C.E. Clauser, Anthropology Branch, 6570th Aerospace Medical Research Laboratories

TABLE VI

COORDINATES OF THE SEGMENT HINGE POINTS AND MASS CENTERS

Hinge Point and Symbol*		Coordinates (Inches)		
		X	Y	Z
Neck	• A	0	0	59.08
Shoulder	• B	0	7.88	56.50
Elbow	• C	0	7.88	43.50
Hip	• D	0	3.30	34.52
Knee	• E	0	3.30	18.72
Mass Center and Symbol*				
Head	○ 1	0	0	64.10
Torso	○ 2	0	0	46.80
Upper Arm	○ 3	0	7.88	50.83
Lower Arm	○ 4	0	7.88	39.20
Hand	○ 5	0	7.88	31.68
Upper Leg	○ 6	0	3.30	27.68
Lower Leg	○ 7	0	3.30	11.80
Foot	○ 8	2.45	3.30	1.37

**Symbols indicated in figure 2*

TABLE VII

MOMENTS OF INERTIA OF THE SEGMENTS FOR TWO POSITIONS*

		Segments†								
		Head	Torso	Upper Arms	Lower Arms	Hands	Upper Legs	Lower Legs	Feet	Total
$I_{x_{cg}}$	Position A	0.0183	1.0000	0.0157	0.0056	0.0004	0.0776	0.0372	0.0006	1.2927
	Position B	0.0183	1.0000	0.0157	0.0044	0.0004	0.0620	0.0372	0.0006	1.2589
mD^2	Position A	1.5114	1.0125	0.2199	0.0405	0.0292	0.4964	1.3114	0.7388	8.1963
	Position B	0.7859	0.0092	0.0932	0.0407	0.0303	0.1496	0.0588	0.1252	1.7907
I_x	Position A	1.5297	2.0125	0.2356	0.0461	0.0296	0.5740	1.3486	0.7394	9.4890
	Position B	0.8042	1.0092	0.1089	0.0451	0.0307	0.2116	0.0960	0.1258	3.0496
$I_{y_{cg}}$	Position A	0.0183	0.9300	0.0157	0.0056	0.0004	0.0776	0.0372	0.0028	1.2269
	Position B	0.0183	0.9300	0.0157	0.0056	0.0004	0.0776	0.0372	0.0028	1.2269
mD^2	Position A	1.5114	1.0125	0.1517	0.0000	0.0137	0.4582	1.2925	0.7361	7.8284
	Position B	0.7950	0.0734	0.0292	0.0002	0.0188	0.1190	0.1015	0.1560	1.7176
I_y	Position A	1.5297	1.9425	0.1674	0.0056	0.0141	0.5358	1.3297	0.7389	9.0553
	Position B	0.8133	1.0034	0.0449	0.0058	0.0192	0.1966	0.1387	0.1588	2.9445
$I_{z_{cg}}$	Position A	0.0124	0.2300	0.0018	0.0008	0.0004	0.0154	0.0037	0.0028	0.2922
	Position B	0.0124	0.2300	0.0018	0.0020	0.0004	0.0310	0.0037	0.0028	0.3258
mD^2	Position A	0.0000	0.0001	0.0682	0.0405	0.0155	0.0382	0.0188	0.0085	0.3797
	Position B	0.0091	0.0642	0.0723	0.0405	0.0195	0.0459	0.0804	0.0420	0.6746
I_z	Position A	0.0124	0.2301	0.0700	0.0413	0.0159	0.0536	0.0226	0.0113	0.6719
	Position B	0.0215	0.2942	0.0742	0.0426	0.0199	0.0769	0.0841	0.0448	1.0004

** Positions A and B are shown in figure 5*
† All values are slug-ft²

Analysis:

The dynamics of a rotating body in space depends primarily upon two factors: the center of mass location of the whole body and the moments of inertia of the whole body about axes through the body center of mass.

The variation of the center of mass of the human body has been studied extensively (ref. 11) and can be accurately predicted for a given body position without difficulty. The center of mass of the model is found to lie 39.09 inches from the floor or 56.6% of the body length. This falls within the 55 to 57.4% range determined experimentally by Dempster (ref. 4) and agrees closely with an average of 55.6% measured by Swearingen (ref. 20) on five living subjects.

Predicting the moments of inertia is somewhat more involved and may be less accurate. Therefore, the mathematical model is analyzed to determine:

a. Which segments have the greatest effect on the total moment of inertia

b. The degree of approximation by representing the segments as geometrical bodies

c. Which segments can be further simplified without a significant loss in accuracy

The first position, standing erect with arms at the sides (position A, figure 5), is considered the normal position. For the second position (position B, figure 5), the arms and legs are drawn up close to the torso to give a near-minimum moment of inertia about the X- and Y-axes. The moments of inertia for position B are calculated in much the same way as for position A and presented in table VII. For this new position, the center of mass moves 7.0 inches toward the head along the Z-axis and 1.9 inches forward along the X-axis.

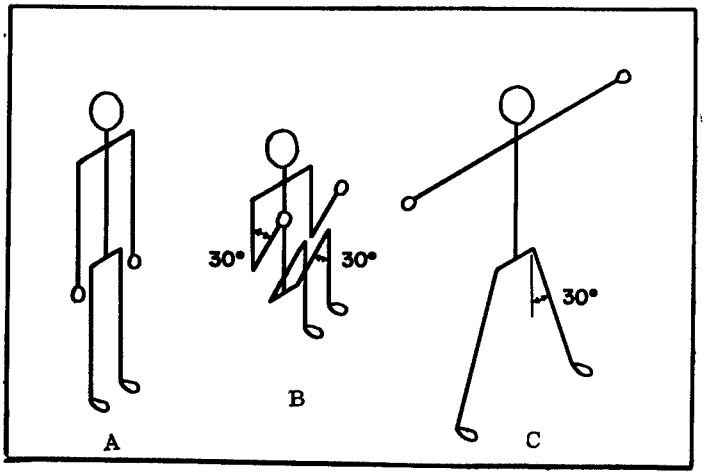

Figure 5. Body Positions

The moment of inertia of the whole body about an axis is given by the sum of the moments of inertia of all segments about that axis. The moment of inertia of each segment of equation 8 consists of two parts which are defined as:

Local Term I_{cg}. — The moment of inertia of the segment about an axis through its center of mass parallel to the given axis.

Transfer Term mD^2. — A quantity given by the product of the mass of the segment times the square of the perpendicular distance between the two parallel axes.

Since the local terms are the most tedious to compute, it is convenient to see what contributions they make toward the total moment of inertia. If the contributions are small, these terms may be neglected. In figure 6, the local and transfer terms for the two positions are compared. Since these quantities are nearly the same about the X- and Y-axes, the X-axis is not indicated.

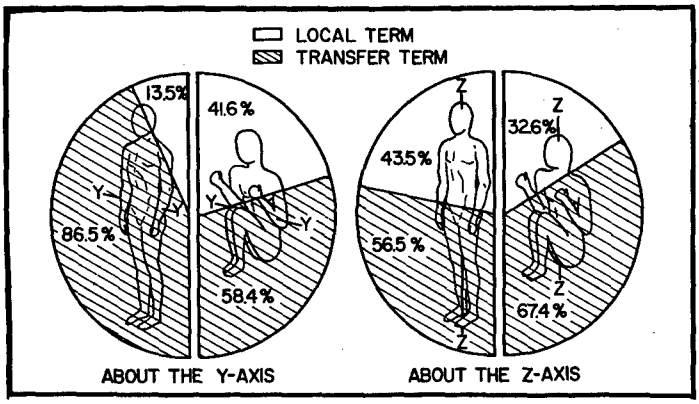

Figure 6. Comparison of Local to Transfer Moment of Inertia Terms (expressed as a percent of the total moment of inertia)

Figures 7 and 8 illustrate the contribution each segment makes toward the total moment of inertia, and what effects each local and transfer term has on the total moment of inertia.

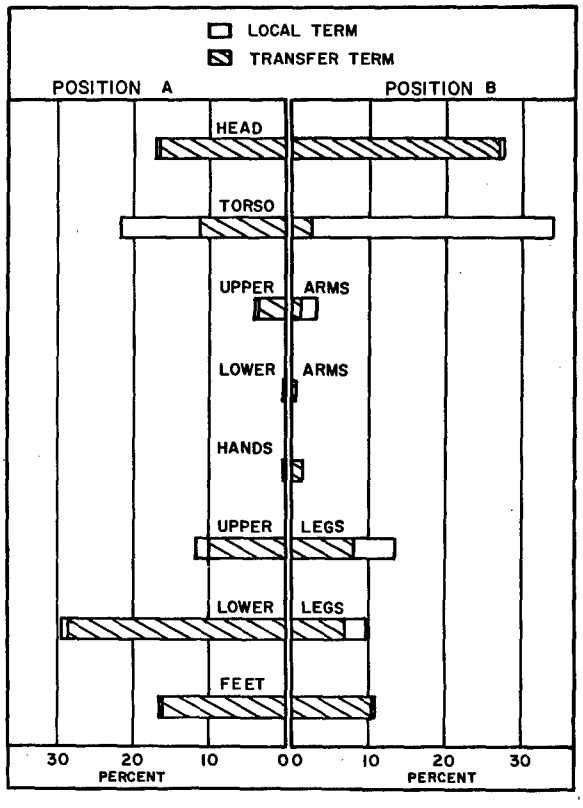

Figure 7. Percent of Total Moment of Inertia about the Y-Axis for Each Segment

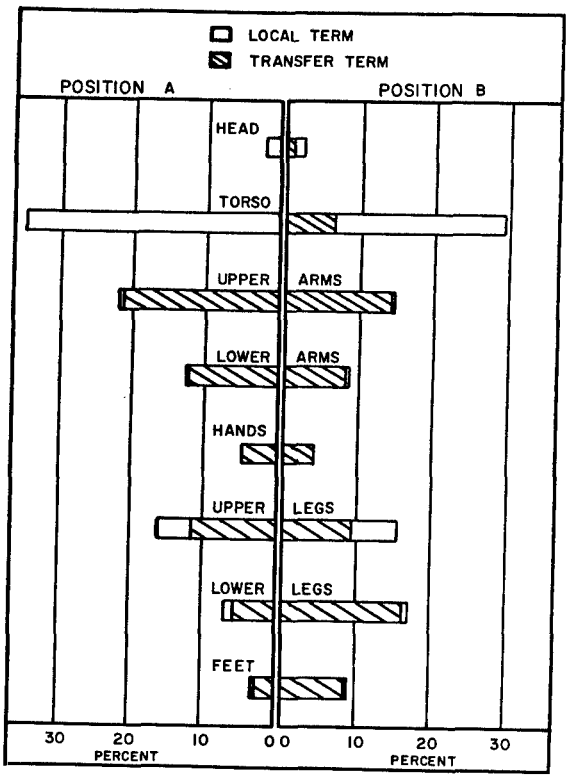

Figure 8. Percent of Total Moment of Inertia about the Z-Axis for Each Segment

Conclusions:

A close look at figures 6, 7, and 8 reveals some important information. In general, the local moment of inertia terms cannot be neglected, particularly about the Z-axis. However, the contribution of the local term for several segments is zero or negligible. Hence, it is unnecessary to compute the local moment of inertia for the hands, lower arms, and feet, since their sum is less than the errors due to simplifying the human body. Further, the geometric representation for the upper arms, upper and lower legs, and head need not be too accurate. For instance, a 33% variation in the moment of inertia of the upper arm would change the total moment of inertia (for position A) about the X-axis only ±0.1%. The total moment of inertia of the torso must be computed with much more care since it may contribute 10% to 35% of the total moment of inertia depending on the axis and position.

Simplified Approach:

Based on the above conclusions, a simplified method is developed for computing the moments of inertia for various body positions. Starting with the moments of inertia for position A computed above as initial conditions (I_{x_0}, I_{y_0}, I_{z_0}), this method yields the moments of inertia for any other position (I_x, I_y, I_z) by taking into account only the changes in the transfer terms and the relative position of the body axis system. This approach greatly simplifies the mathematics, and, although it neglects the changes in the local terms, there is only a slight reduction in accuracy.

The moment of inertia of the model (consisting of "p" masses or segments) about the X-axis for position A is given by:

$$I_{x_o} = \sum_{i=1}^{p} I_{x i_{o_{cG}}} + \sum_{i=1}^{p} m_i (Y_{i_o}^2 + Z_{i_o}^2) \tag{9}$$

When the body position changes, the moment of inertia (I'_{x_o}) about the same axis is given by:

$$I'_{x_o} = \sum_{i=1}^{p} I_{x i_{cG}} + \sum_{i=1}^{p} m_i (Y_i^2 + Z_i^2) \tag{10}$$

To find the moment of inertia about a parallel axis through the center of mass for this new position, the Parallel Axis Transfer Theorem is used:

$$I'_{x_o} = I_x + m_{tot}(\overline{Y}^2 + \overline{Z}^2) \tag{11}$$

Now:

$$I_x + m_{tot}(\overline{Y}^2 + \overline{Z}^2) = \sum_{i=1}^{p} I_{x i_{cG}} + \sum_{i=1}^{p} m_i (Y_i^2 + Z_i^2) \tag{12}$$

Subtracting equation 9 from equation 12:

$$I_x + m_{tot}(\overline{Y}^2 + \overline{Z}^2) - I_{x_o} = \sum_{i=1}^{p} I_{x i_{cG}} + \sum_{i=1}^{p} m_i (Y_i^2 + Z_i^2)$$

$$- \sum_{i=1}^{p} I_{x i_{o_{cG}}} - \sum_{i=1}^{p} m_i (Y_{i_o}^2 + Z_{i_o}^2) \tag{13}$$

Assuming the local terms do not change:

$$\sum_{i=1}^{p} I_{x i_{cG}} = \sum_{i=1}^{p} I_{x i_{o_{cG}}} \tag{14}$$

and equation 13 becomes:

$$I_x = I_{x_o} - \sum_{i=1}^{p} m_i \left[(Y_{i_o}^2 + Z_{i_o}^2) - (Y_i^2 + Z_i^2) \right] - m_{tot}(\overline{Y}^2 + \overline{Z}^2) \tag{15}$$

Now if only "n" masses change position, the coordinates of the "p-n" masses will remain the same and will cancel out. Then:

$$I_x = I_{x_o} - \sum_{i=1}^{n} m_i \left[(Y_{i_o}^2 + Z_{i_o}^2) - (Y_i^2 + Z_i^2) \right] - m_{tot}(\overline{Y}^2 + \overline{Z}^2) \tag{16}$$

In a similar manner the equations for the moments and products of inertia about the other axes are found to be (ref. 8):

$$I_Y = I_{Y_o} - \sum_{i=1}^{n} m_i \left[(X_{i_o}^2 + Z_{i_o}^2) - (X_i^2 + Z_i^2)\right] - m_{tot}(\overline{X}^2 + \overline{Z}^2) \tag{17}$$

$$I_Z = I_{Z_o} - \sum_{i=1}^{n} m_i \left[(X_{i_o}^2 + Y_{i_o}^2) - (X_i^2 + Y_i^2)\right] - m_{tot}(\overline{X}^2 + \overline{Y}^2) \tag{18}$$

$$I_{XY} = \sum_{i=1}^{n} m_i \left[(X_i Y_i) - (X_{i_o} Y_{i_o})\right] - m_{tot}(\overline{X}\,\overline{Y}) \tag{19}$$

$$I_{YZ} = \sum_{i=1}^{n} m_i \left[(Y_i Z_i) - (Y_{i_o} Z_{i_o})\right] - m_{tot}(\overline{Y}\,\overline{Z}) \tag{20}$$

$$I_{ZX} = \sum_{i=1}^{n} m_i \left[(Z_i X_i) - (Z_{i_o} X_{i_o})\right] - m_{tot}(\overline{Z}\,\overline{X}) \tag{21}$$

where:

$$\overline{X} = \frac{1}{m_{tot}} \sum_{i=1}^{n} m_i (X_i - X_{i_o}) \tag{22}$$

$$\overline{Y} = \frac{1}{m_{tot}} \sum_{i=1}^{n} m_i (Y_i - Y_{i_o}) \tag{23}$$

$$\overline{Z} = \frac{1}{m_{tot}} \sum_{i=1}^{n} m_i (Z_i - Z_{i_o}) \tag{24}$$

$m_i \equiv$ mass of the ith segment

$X_i Y_i Z_i \equiv$ coordinates of the center of mass of the ith segment after some change

$X_{i_o} Y_{i_o} Z_{i_o} \equiv$ coordinates of the centers of mass of the ith segment before some change

$m_{tot} \equiv$ total mass

and "n" is the number of segments which change positions from the initial conditions. For instance, if one arm is raised from position A, the center of mass of the upper and lower arm and hand will change. Three segments are involved, so n = 3 and m_1 might refer to the mass of the upper arm, m_2 to the mass of the lower arm, m_3 to the mass of the hand.

Equations 22, 23, and 24 are exact and will always yield the coordinates of the new center of mass with respect to the center of mass location for position A.

Up to this point, nothing has been said about products of inertia (I_{xy}, I_{yz}, I_{zx}). While the body axis system in position A coincides with the principal axes of inertia and there are no products of inertia, this will not be true in general. Principal axes of inertia are defined as a set of orthogonal axes about which the products of inertia are zero. In fact, in position B the principal axes are tilted forward (rotated about the Y-axis in the negative direction) approximately 8^c from the body axes. Therefore, a product of inertia, I_{zx}, exists.

From equations 16, 17, and 18 the moments of inertia of the model are computed for positions B and C. These results are compared with exact results taking the local terms into account in table VIII.

TABLE VIII

COMPARISON OF MOMENTS OF INERTIA FROM EXACT AND APPROXIMATE METHODS

	Moments of Inertia (Slug-ft^2)					
	I_x for Position		I_y for Position		I_z for Position	
	B	C	B	C	B	C
Exact Method	3.0496	12.225	2.9445	8.8430	1.0004	3.6210
Approximate Method	3.0845	12.225	2.9445	8.7917	0.9668	3.5356
Percent Error	+1.14	0.00	0.00	-0.58	-3.36	-2.36

The approximate method yields exact results for I_x, position C, and I_y, position B. This occurs because there is no change in the local moment of inertia terms, $I_{x_{CG}}$ for position C and $I_{y_{CG}}$ for position B.

Thrust Misalignment

For a man (initially at rest) to move between two points in space, some external force must be applied. If translation is to take place without rotation, the resultant force must act through the man's center of mass. Since man is not a rigid body, flexing and bending the various appendages will cause the center of mass to change position with respect to the body. Therefore, it is unlikely that any single force device would act through the center of mass. The case of a single force device rigidly attached to the space worker so that a constant force is applied, not through the center of mass, provides an interesting space dynamics problem. It has practical application to any propulsion and stabilization device since thrust misalignment might occur during a malfunction of the system or from poor operator technique.

Consider a thrust misalignment which produces a constant moment about one of the principal moment of inertia axes. If $I_X = I_Y$ and the moment is applied about the Y-axis, the resulting motion will be a spin about the Y-axis and the center of mass will move in the plane of the XZ-axes. Proof of this statement and complete derivation of the equations of motion are given in Appendix B. Even for this restricted two-dimensional problem, a closed form solution could not be achieved. However, the equations of motion were nondimensionalized and, by applying the Runge-Kutta Method (ref. 16), a machine solution was achieved on the AFIT IBM 1620 Digital Computer. A nondimensional plot of the velocities is given in figure 14 and the trajectory in figure 15.

For this special case of plane motion, the trajectory always approaches a straight line which is inclined 45° to the original heading. While the angular velocity increases as long as the misaligned thrust is applied, the linear velocity of the center of mass approaches a limit as can be seen in figure 14.

As an example, if the USAF mean man is subjected to a 10-pound thrust misaligned 7.0 inches along the Z-axis, in the direction of the X-axis, a constant magnitude moment of 70 in-lbs is applied about the Y-axis. When the values of moments of inertia for position B are taken as principal moments of inertia, a solution to this problem (see the example problem at the end of Appendix B) indicates that at 5 seconds the man will have been accelerated to an angular velocity of 96 rpm; he will have completed four revolutions, and reached a linear velocity of 1.6 ft/sec. After 10 seconds, he will have made almost 16 revolutions, and will be rotating at a rate of 191 rpm while moving at a rate of 1.7 ft/sec.

Maneuvering

A problem somewhat similar to the misaligned thrust problem is controlled rotation or maneuvering. The space worker will be equipped with a propulsion and stabilization unit to maneuver around his or other space vehicles. The question arises: Is there an optimum way to perform a particular maneuver?

In this section a very simplified problem is analyzed with the objective of showing that there is a considerable variation in the fuel required to execute a given maneuver. The optimum condition is achieved when the maneuver is completed with minimum fuel consumption.

Consider the following hypothetical problem. The space worker is moving with a constant initial velocity, V_0 (relative to the space vehicle), and he desires to make a 90° change in his flight path. How does he direct his thrust (thrust vector) so that, after a period of time, T, he is moving at the same rate, V_0, perpendicular to the original heading, and a minimum amount of fuel is consumed?

Three Thrust Programs:

Three thrust programs are analyzed based on the following assumptions:

a. The man (including the maneuvering unit) is a mass particle.

b. The period, T, of thrust application is small so that the mass, m, of the system is considered constant.

These assumptions reduce the problem to one of particle dynamics and neglect problems associated with the orientation of the man and how the particular thrust program is achieved. In all three problems the same thrust is applied although the length of time and the direction vary. Since fuel consumption will depend solely upon the time applied for a constant magnitude thrust, the problem becomes one of determining the minimum thrusting time.

Case I. — First consider the case in which the thrust, F_o, is applied in direct opposition to the initial motion until this motion ceases. Then F_o is applied perpendicular to the original flight direction until a speed, V_o, is reached. From Newton's Equation:

$$F = \frac{d}{dt}(mV) \tag{25}$$

and integrating with respect to time, $F = -F_o$:

$$-F_o t = mV + C \tag{26}$$

Applying the initial conditions, $t = 0$ and $V = V_o$:

$$t = \frac{m}{F_o}(V_o - V) \tag{27}$$

Now at $t = t_1$, $V = 0$, so that the time to stop is t_1:

$$t_1 = \frac{mV_o}{F_o} \tag{28}$$

By the same approach, the time to accelerate to V_o again is t_2:

$$t_2 = \frac{mV_o}{F_o} \tag{29}$$

Therefore, the total thrusting time, T, is given by:

$$T = t_1 + t_2 = \frac{2mV_o}{F_o} \tag{30}$$

If the initial velocity is in the X-direction and the final velocity is in the Y-direction, the velocity components, V_x and V_y, will vary as shown in figure 9, for Case I. While no values are shown for the plots in figure 9, all are drawn to the same scale so that the results may be compared.

Case II. — Suppose the decelerating force, F_o, is applied at a 45° angle in opposition to the initial motion so that one component of the force, $F_x = -0.707F_o$, acts in direct opposition to the original motion. Then the other component, $F_y = 0.707F_o$, will act normal to the initial flight path. Writing Newton's Equation in component form:

$$F_x = \frac{d}{dt}(mV_x) \tag{31}$$

and integrating with respect to time, $F_x = -0.707F_o$:

$$-0.707F_o t = mV_x + C \tag{32}$$

Applying the initial conditions at $t = 0$, $V_x = V_o$:

$$t = \frac{m}{0.707F_o}(V_o - V_x) \tag{33}$$

Now at $t = t_1$ and $V_x = 0$, the time to stop is t_1:

$$t_1 = 1.414 \frac{mV_o}{F_o} \tag{34}$$

By a similar approach:

$$t_2 = 1.414 \frac{mV_o}{F_o} \tag{35}$$

Now F_x and F_y are applied simultaneously so that the complete maneuver is completed during time, t_1, or:

$$t_1 = t_2 = T \tag{36}$$

The variations of V_x and V_y are shown in figure 9.

Case III. —Consider now a case in which the thrust is applied normal to the flight path until the man has completed a 90° turn. Then the thrust, F_o, will be equal to the centrifugal force or:

$$F_o = \frac{mV_o^2}{\rho} \tag{37}$$

where ρ is the radius of curvature. Since there is no force applied tangent to the flight path, V_o remains constant and the flight path is an arc of a circle of radius, ρ. The arc (S) will be one-fourth of a circle.

The time to cover this distance is given by:

$$t = \frac{S}{V_o} = \frac{(\pi/2)\rho}{V_o} = \frac{\pi \rho}{2V_o} \tag{38}$$

But from equation 37:

$$\rho = \frac{mV_o^2}{F_o} \tag{39}$$

so that equation 38 becomes:

$$t = \frac{\pi mV_o}{2F_o} \tag{40}$$

and since $t = T$:

$$T = 1.57 \frac{mV_o}{F_o} \tag{41}$$

The variation of the X- and Y-components of the velocity are shown in figure 9 also.

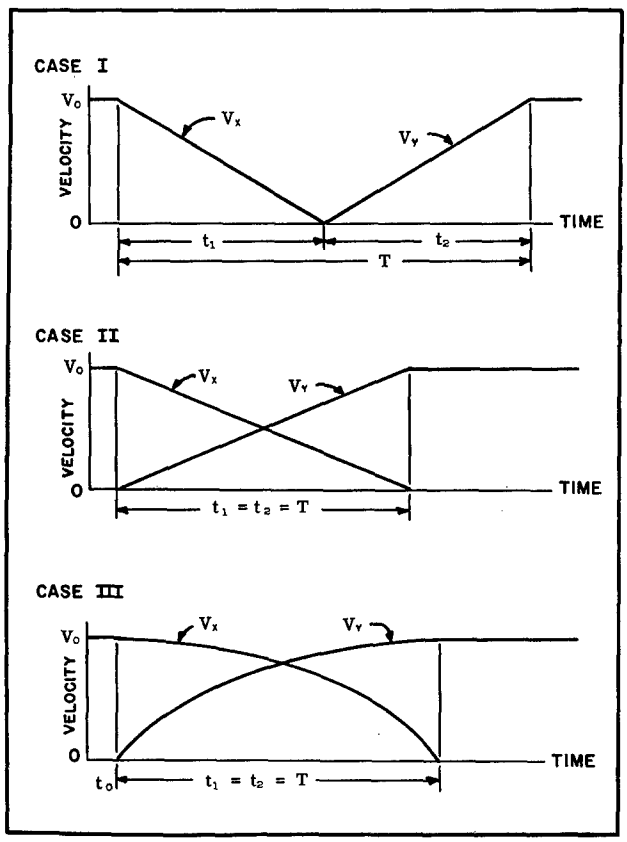

Figure 9. Velocity Versus Time for Three Turning Maneuvers

Conclusions:

While only three cases of the above plane motion problem are considered, some significant differences in maneuvering times are noted. If Case II is taken as a standard of comparison, we see that Case I takes 41.5% longer to execute the 90° turn and Case III takes 11.0% longer. In terms of fuel consumption, Case I appears to be quite impractical. No restriction is made on the distance required to complete the maneuver. Since this distance will vary for the three cases, any such restriction would require a reanalysis of these thrust programs.

Free-Body Dynamics

Free-floating man cannot, without some external force, displace his center of mass. However, he can change his attitude by properly manipulating his appendages. Nine maneuvers have been proposed by Kulwicki (ref. 14) for achieving self-rotation.

In Appendix C a more general equation of motion is derived based on conservation of angular momentum (i.e., in the absence of any external force, the total angular momentum remains constant). This derivation is based on an analysis of spacecraft docking dynamics by Grubin (ref. 10). While no particular maneuvers are described, the equation presented and the method of its development can be applied to a wide range of free-body dynamics problems.

As an example of a free-body dynamics problem, consider the free-floating space worker in an initial position with both arms raised vertically above his head. If he swings both arms (parallel to each other) forward an angle ν, his torso will be tilted backward an angle γ. The equation for the change in body attitude (developed in Appendix C) becomes for the USAF mean man:

$$\gamma = \frac{\nu}{2} - 0.86758 \arctan(0.86507 \tan \frac{\nu}{2}) \tag{42}$$

or for each revolution of the arms, $\gamma = 23.8°$.

Stability of Rotation

The moment-free motion of an unsymmetrical rigid body with principal moments of inertia—I_x, I_y, and I_z—is an unsteady periodic precession and nutation about the resultant angular momentum vector which is fixed in space. Steady rotation exists only about the principal axis of maximum or minimum moment of inertia, the principal axis of intermediate moment of inertia being unstable. Rotation about the axis of maximum or minimum moment of inertia is considered stable; that is, if the spin axis deviates slightly from the resultant angular momentum vector, there is no tendency for this deviation to grow. This can be said only for a perfectly rigid body in the absence of external moments (ref. 22).

Consider a nonrigid body rotating in space. Because of energy dissipation, the kinetic energy of rotation will decrease with time. The equation for the decrease in kinetic energy, $\dot{T}$, is given by Thomson (ref. 22) for a body of revolution ($I_x = I_y$), with principal moments of inertia—I_x, I_y, and I_z — to be:

$$\dot{T} = I_z \omega_o^2 \left(\frac{I_z}{I_x} - 1\right)(\sin \alpha \cos \alpha)\dot{\alpha} \tag{43}$$

where:

$\omega_o \equiv$ initial spin velocity

$\alpha \equiv$ angle between the spin axis and the angular momentum vector

$\dot{\alpha} \equiv$ rate at which the angle α is changing

Since $\dot{T}$ is always negative, $\dot{\alpha}$ is negative for $\frac{I_z}{I_x} > 1$ and positive for $\frac{I_z}{I_x} < 1$. If I_z is the minimum principal moment of inertia, then $\frac{I_z}{I_x}$ is less than one, $\dot{\alpha}$ is positive, and α is increasing. Thus, the principal axis of minimum moment of inertia is one of unstable equilibrium, and a small deviation of the spin axis from the angular momentum vector will increase due to energy dissipation. Man is certainly not a rigid body and, under cyclic stresses induced by gyroscopic precession, energy will be dissipated.

Since we have shown that rotation about the axis of minimum inertia may be unstable, there is reason to believe that weightless man may possess only one stable axis of rotation. This is rotation about the principal axis of maximum moment of inertia. If he is initially rotating about the principal axis of maximum inertia, weightless man could change the axis of rotation by moving his limbs. For this case, we can say that he would possess no stable axis of rotation.

Application of a Torque

Applying a torque to some relatively fixed object will be part of the function of the space worker performing assembly and repair tasks. The resulting reaction of the free-floating worker will depend upon how the torque is applied (i.e., the magnitude of the torque as it varies over a short interval of time). This reaction has been studied by Dzendolet (ref. 7)—however, without exact knowledge of the nature of the torque input, and under normal 1-G conditions.

In this section a general equation of motion is developed and solved based on the assumption (experimentally validated and described in the next section for a short-duration, impulselike torque) that the torque input varies as a half-sine wave. Then:

$$M(t) = M_M \sin \frac{\pi t}{T} \tag{44}$$

where:

$M(t)$ ≡ torque as a function of time
M_M ≡ maximum torque achieved
T ≡ period of torque application
t ≡ time

For rotation about one of the principal axes of inertia we have:

$$I\dot{\omega} = M(t) = M_M \sin \frac{\pi t}{T} \tag{45}$$

where:

I ≡ moment of inertia
$\dot{\omega}$ ≡ angular acceleration

Assuming I is constant, we have, after integrating:

$$I\omega = \frac{M_M T}{\pi}\left(1 - \cos\frac{\pi t}{T}\right) \tag{46}$$

and at t = T:

$$I\omega = 2\frac{M_M T}{\pi} \tag{47}$$

$$\omega = \frac{2M_M T}{\pi I} \tag{48}$$

Equation 48 then yields the angular velocity at the end of the torque application period.

Suppose the USAF mean man reaches overhead to grasp a valve handle (for instance, a fuel shut-off valve on the space station). What will happen if he attempts to close the valve with a sudden twist, and the valve is frozen and does not turn?

Assume the following conditions exist:

a. The space worker is unrestrained.

b. The torque is applied about the Z-axis (a principal axis).

If the principal moment of inertia about the Z-axis is:

$$I_z = 0.55 \text{ slug-ft}^2$$

and the maximum torque developed is 2.71 ft-lbs over a period of 1.1 seconds, then, by equation 48:

$$\omega = 0.6366\frac{(2.71)(1.1)}{(0.55)}$$

$$= 3.45 \text{ radians/second}$$
$$= 32.9 \text{ rpm}$$

Hence, the space worker will be spinning about the Z-axis at a rate of 32.9 rpm after the torque application.

EXPERIMENTAL RESULTS

The last phase of this study was concerned with experimental validation of some of the analytical results derived in the previous section. Two experiments were conducted by personnel of Crew Stations Branch of the Behavioral Sciences Laboratory, under weightless conditions. Zero-gravity conditions were achieved for periods up to 30 seconds in a USAF KC-135 jet transport, flying parabolic trajectories. All experiments were recorded on motion picture film.

Stability Experiment

Object:

This experiment was designed to demonstrate instability of a nonrigid body rotating about the axis of minimum moment of inertia.

Procedure:

The free-floating subject (holding position A, figure 5, as rigidly as possible) was spun about the Z-axis by means of a rope wound around the waist. Part A: The subject held position A throughout the free-rotation period. Part B: Two to three seconds after spin-up, the subject raised one knee to induce a wobble to the spin.

Results and Discussion:

Part A: Spins up to 120 rpm were achieved and appeared stable for the short impact-free periods (5-8 seconds).

It was intended to perform the spins so that the body Z-axis was parallel to the pitch axis of the aircraft, to eliminate any cross-coupling effects due to the rotating reference system. However, there were practical difficulties in this method, and, to get satisfactory spins and photographic coverage, the spins were imparted with the body Z-axis parallel to the longitudinal axis of the aircraft. The cross-coupling effects apparently were small as no significantly different results could be detected between the two spin axis orientations.

Part B: When one knee was flexed, a wobble in the spin did result, but the test area was not large enough to allow the subject to tumble freely without striking parts of the aircraft. Maximum impact-free periods from 5 to 6 seconds were not long enough to conclusively demonstrate a change to stable rotation about the X- or Y-axes. A typical run is shown in figure 10. The photographs were taken in sequence, left to right, at 0.5-second intervals.

On two of the runs the subject spread both arms and legs during the impact-free period and a decrease in rpm from 2.5 to 1 was observed.

Torque Experiment

Object:

This experiment was designed to determine the nature of a short-duration, impulselike torque which weightless (and hence frictionless) man can exert on a rigidly mounted handle.

Apparatus:

A small beam fitted with strain gages was attached inside a tubular handle, 6 inches long and 3/4 inch in diameter. The strain gage outputs were fed into the aircraft oscillograph so that strains produced deflections which were plotted as functions of time. The system was calibrated so that the deflections could be interpreted as torque applied to the handle.

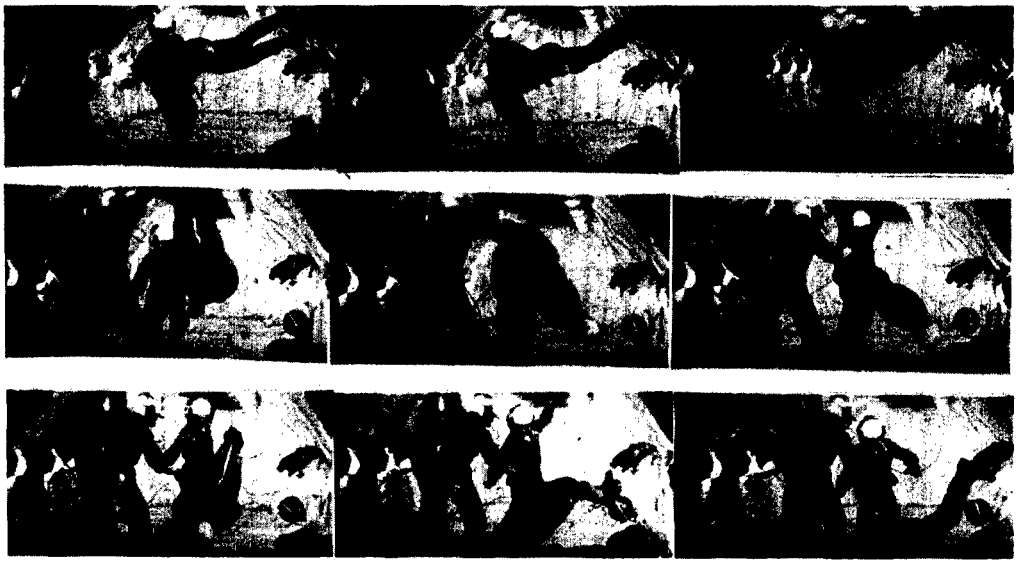

Figure 10. Sequence Photographs of the Free Rotation of a Subject Initially Spun About a Head-to-Toe Axis (taken at 0.5-second intervals)

Procedure:

The weightless subject grasped the handle with his right hand and with near-maximum strength applied a quick counterclockwise torque of approximately 1-second duration. Part A: During the torque application and resulting rotation, the subject held body position A, except that the right arm was extended over the head to grasp the handle. Part B: During the torque application and resulting rotation, the subject held a sitting body position (Indian fashion with legs crossed) and grasped the torque handle with the hand, arm extended, directly in front of the torso about shoulder level.

Results and Discussion:

Two typical torque versus time plots are shown in figure 11. As can be readily seen, these curves closely resemble a half-sine wave. From equation 48 developed in the previous section, the resultant angular velocity can be calculated when the moment of inertia is known. The moment of inertia is found by the methods of the first phase. These velocities are compared in table IX to actual velocities determined from motion pictures of the experiment. The greatest difference arises from not being able to determine the exact axis of rotation (or direction of the angular velocity vector), and, hence, the moment of inertia about that axis. This error could be as large as ±10%. Also, angular velocities determined by photographic means can vary ±2%. The maximum error considering all sources should be less than ±15%.

Conversely, the moment of inertia can be calculated from equation 48 when the measured angular velocity is used.

The maximum torques achieved during weightlessness averaged (for 6 runs with 2 subjects) 66.6% of the peak torques under static 1-G conditions.

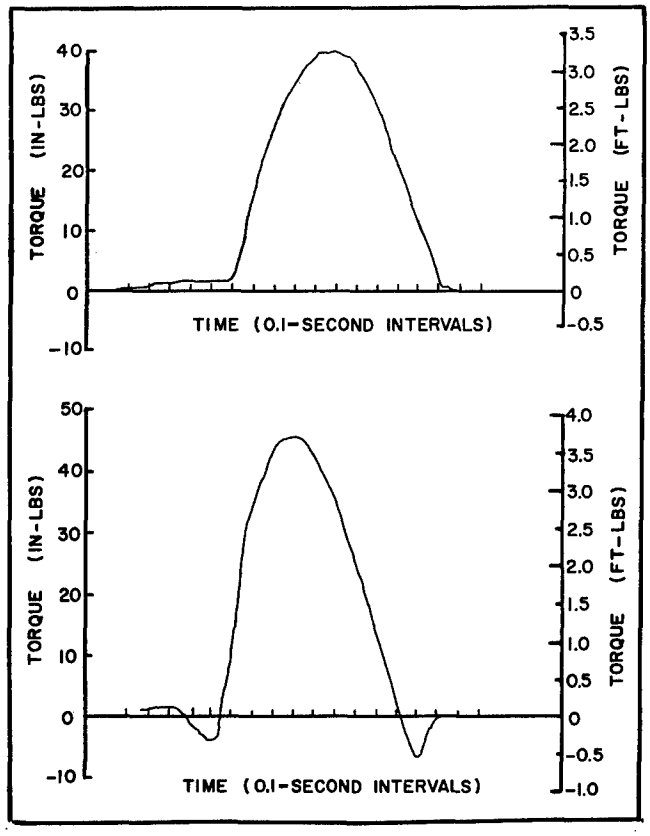

Figure 11. Typical Plots of the Torque That Man Can Exert While Weightless as a Function of Time

TABLE IX

COMPARISON OF ANALYTICAL AND EXPERIMENTAL ANGULAR VELOCITIES FROM THE TORQUE APPLICATION EXPERIMENT

Run Number	T (seconds)	M_M (ft-lbs)	I (slug-ft^2)	ω Analytical (rad/sec)	ω Experimental (rad/sec)	Error* (%)
2	1.10	2.71	0.55	3.45	3.59	-3.9
5	1.00	3.34	1.05	2.02	1.86	+8.6
6	0.88	3.75	1.05	1.99	1.86	+7.0

** Analytical results compared to the experimental results*

CONCLUDING STATEMENTS AND RECOMMENDATIONS FOR FUTURE STUDY

The mathematical model developed to represent weightless man is based on the biomechanical properties of the human body. Since there are no methods of determining many of these properties accurately from a living subject, statistical data is used which is a function of the total body weight. Body dimensions, however, can be measured for any given living subject.

In the first phase the transfer moment of inertia terms are shown to be a very important part of the total moment of inertia. Since the transfer term, mD^2, depends upon the square of the distance between the mass and the inertia axis, it is more sensitive to variations in distance than to mass variations. Therefore, a model based on anthropometry of a given subject will reflect the dynamic response characteristics of that subject.

The statistical methods of estimating the other biomechanical properties (mass, mass center, and density) presented in refs. 1, 2, 4, and 6 are being refined and made more adaptable to living subjects by the Anthropology Branch of the Behavioral Sciences Laboratory. Hence, in the near future, more accurate methods of determining these properties from a living subject may be available.

The assumption that the human body consists of 14 rigid and homogeneous segments is a convenient, but not too realistic, idealization. However, for the intended application of the model to dynamics problems facing weightless man, this assumption will not produce any great inaccuracies. For example, first space suits will be equipped with large environmental backpacks and/or propulsion and stabilization systems which will not allow much flexing of the back. Therefore, the assumption that the torso is rigid actually fits the physical situation.

A simplified approach is presented for calculating the new center of mass location and moments of inertia when the model's position deviates from the standing straight position (figure 5, position A). The resulting equations can be easily represented electrically so that the human system parameters can be programed into an analog simulator of a propulsion and stabilization system for the space maintenance worker.

The model is based on a nude man to establish unencumbered man's baselines (without hardware). Hardware, such as the space suit, magnetic shoes, environmental pack, etc., can be included after man's basic response characteristics have been investigated.

The analytical results are qualitative in nature and are intended to offer a first approximation to the selected problems. The simplifying assumptions are not, in general, too restrictive. For instance, the assumption that man is a body of revolution so that $I_x = I_y$ is almost satisfied for many positions (note that, for position A, $I_x = 1.046 I_y$ or I_x is 4.6% greater than I_y). Each restricted problem has practical application to the actual problems of the space worker. In summary, these problems demonstrate the requirement for a propulsion and stabilization device for the space worker.

The experimental results are preliminary in nature. However, the stability experiment cannot be used to verify the analytical results because of the short impact-free rotation period. The torque experiment did successfully demonstrate the practicality of the apparatus and the approach used. More data is required, however, before the analytical results can be conclusively established.

BIBLIOGRAPHY

1. Barter, J. T., Estimation of the Mass of Body Segments, WADC Technical Report 57-260, Wright Air Development Center, Wright-Patterson Air Force Base, Ohio, April 1957, ASTIA No. 118 222.

2. Braune, W., and O. Fischer, Treatises of the Mathematical-Physical Class of the Royal Academy of Sciences of Saxony, Number 7, Leipzig, 1889. (U. S. Army Air Forces, Air Materiel Command Translation No. 379, Wright Field, Dayton, Ohio.)

3. Celentano, J. T., and H. S. Alexander, The Use of Tools in Space - An Empirical Approach, IAS Paper No. 61-145-1839, Institute of the Aerospace Sciences, New York, 1961.

4. Dempster, W. T., Space Requirements of the Seated Operator, WADC Technical Report 55-159, Wright Air Development Center, Wright-Patterson Air Force Base, Ohio, July 1955.

5. Downey, G. L., and G. M. Smith, Advanced Dynamics for Engineers, International Textbook Company, Scranton, Pennsylvania, 1960.

6. Duggar, B. C., "The Center of Gravity of the Human Body," Human Factors, Vol 4, pp 131-148, June 1962.

7. Dzendolet, E. and J. F. Rievley, Man's Ability to Apply Certain Torques While Weightless, WADC Technical Report 59-94, Wright Air Development Center, Wright-Patterson Air Force Base, Ohio, April 1959.

8. Grantham, W. D., Effects of Mass-Loading Variations and Applied Moments on Motion and Control of a Manned Rotating Space Vehicle, NASA Technical Note D-803, National Aeronautics and Space Administration, Washington, D. C., May 1961, ASTIA No. 255 528.

9. Griffin, J. B., F. T. Gardner, and M. L. Barnett, "A Discussion of the Design of a Propulsion and Stabilization System for Man in a Cosmonotic Environment," Proceedings of the National Specialists Meeting on Guidance and Control of Aerospace Vehicles, pp 135-144, Institute of the Aerospace Sciences, New York, 1960.

10. Grubin, C., Docking Dynamics for Rigid-Body Spacecraft, IAS Paper No. 62-43, Institute of the Aerospace Sciences, New York, 1962.

11. Hansen, R., D. Y. Cornog, and H. T. E. Hertzberg, Annotated Bibliography of Applied Physical Anthropology in Human Engineering, WADC Technical Report 56-30, Wright Air Development Center, Wright-Patterson Air Force Base, Ohio, May 1958.

12. Hertzberg, H. T. E., G. S. Daniels, and E. Churchill, Anthropometry of Flying Personnel-1950, WADC Technical Report 52-321, Wright Air Development Center, Wright-Patterson Air Force Base, Ohio, September 1954.

13. Hudson, R. G., The Engineers' Manual (Second Edition), pp 89-94, John Wiley and Sons, Inc., New York, 1939.

14. Kulwicki, P. V., E. J. Schlei, and P. L. Vergamini, Weightless Man: Self-Rotation Techniques, AMRL-TDR-62-129, 6570th Aerospace Medical Research Laboratories, Aerospace Medical Division, Wright-Patterson Air Force Base, Ohio, October 1962.

15. Petrov, V., Artificial Satellites of the Earth, p 124, Hindustan Publishing Corp., Delhi, India, 1960.

16. Scarborough, J.B., Numerical Mathematical Analysis (Fourth Edition), Johns Hopkins Press, Baltimore, Md., 1950.

17. Seale, L.M., and R.E. Flexman, "Research on a Self-Maneuvering Unit for Orbital Workers," Proceedings of the IAS Aerospace Support and Operations Meeting, Institute of the Aerospace Sciences, New York, 1961.

18. Simons, J.C., and M.S. Gardner, Self-Maneuvering for the Orbital Worker, WADD Technical Report 60-748, Wright Air Development Division, Wright-Patterson Air Force Base, Ohio, December 1960.

19. Simons, J.C., and W. Kama, A Review of the Effects of Weightlessness on Selected Human Motions and Sensations, Presented at the AGARD-NATO Aero Space Medical Panel Meeting, Paris, France, 6570th Aerospace Medical Research Laboratories, Aerospace Medical Division, Wright-Patterson Air Force Base, Ohio, April 1962, AD 282 116.

20. Swearingen, J.J., Determination of Centers of Gravity of Man, Final Report United States Navy Contract NAonr 104-51, Civil Aeronautics Medical Research Laboratory, CAA Center Oklahoma City, Oklahoma, 1953.

21. Taylor, C.L., and W.V. Blockley, "Crew Performance in a Space Vehicle," in Space Technology, edited by Howard S. Seifert, pp 30-37, John Wiley and Sons, New York, 1959.

22. Thomson, W.T., Introduction to Space Dynamics, John Wiley and Sons, Inc., New York, 1961.

APPENDIX A

PARAMETRIC STUDY OF THE CENTROID LOCATION AND MOMENTS OF INERTIA OF A FRUSTUM

The frustum of a right circular cone is chosen to represent the upper and lower arms and legs because its centroid can be made to coincide with the centroid of the segment it represents. The segments of the body are assumed to be bodies of revolution with known centroid locations. The location of the centroid becomes an important parameter in defining the properties of the frustum. This appendix presents a derivation of the equations for the centroid location and moments of inertia of a frustum. The equations for the moments of inertia are then expressed in much simpler form in terms of the centroid location. The mass, length, and density of the frustum are left as parameters.

Centroid of a Frustum of a Right Circular Cone

The centroid of the body shown in figure 12 is given by:

$$\overline{Y} = \frac{\int Y dm}{\int dm} \tag{A-1}$$

where:

$$dm = \delta \pi X^2 dY \tag{A-2}$$

and δ is the density (assumed to be constant at every point in the body). Then, for a frustum of length, ℓ, and mass, m, we have:

$$m = \int_0^{\ell} dm = \delta \pi \int_0^{\ell} X^2 dY \tag{A-3}$$

for:

$$X = R - \frac{(R - r)\, Y}{\ell} \tag{A-4}$$

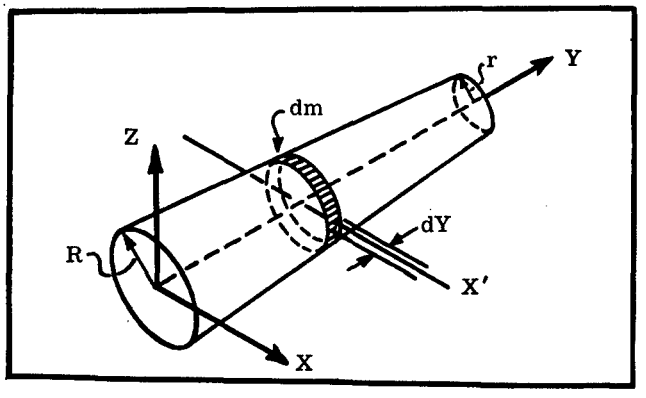

Figure 12. Frustum of a Right Circular Cone

Substituting equation A-4 into equation A-3 and integrating, we have:

$$m = \frac{\delta \pi \ell}{3}(R^2 + Rr + r^2) \tag{A-5}$$

Evaluating the numerator of equation A-1 between the limits from 0 to ℓ, we have, after substituting in equation A-2:

$$\int_o^\ell Ydm = \delta\pi \int_o^\ell YX^2 dY \tag{A-6}$$

$$= \frac{\delta \pi \ell^2}{12}(R^2 + 2Rr + 3r^2) \tag{A-7}$$

Substituting equations A-3 and A-7 into A-1, we have:

$$\overline{Y} = \frac{\ell}{4}\left(\frac{R^2 + 2Rr + 3r^2}{R^2 + Rr + r^2}\right) \tag{A-8}$$

$$= \frac{\ell}{4}\left[\frac{1 + 2\left(\frac{r}{R}\right) + 3\left(\frac{r}{R}\right)^2}{1 + \left(\frac{r}{R}\right) + \left(\frac{r}{R}\right)^2}\right] \tag{A-9}$$

$$= \frac{\ell}{4}\left(\frac{1 + 2\mu + 3\mu^2}{1 + \mu + \mu^2}\right) \tag{A-10}$$

where:

$$\mu = \frac{r}{R} \tag{A-11}$$

Introducing now the nondimensional location at the centroid:

$$\eta = \frac{\overline{Y}}{\ell} \tag{A-12}$$

we have:

$$\eta = \frac{1}{4}\left(\frac{1 + 2\mu + 3\mu^2}{1 + \mu + \mu^2}\right) \tag{A-13}$$

or:

$$\mu = \frac{4\eta - 1}{1 - 2\eta \pm \sqrt{-12\eta^2 + 12\eta - 2}} \tag{A-14}$$

When r = 0 the frustum becomes a right circular cone. When r = R the frustum becomes a right circular cylinder. The ratio, $\frac{r}{R}$, will vary so that:

$$0 \leq \mu \leq 1 \tag{A-15}$$

and:

$$\tfrac{1}{4} \leq \eta \leq \tfrac{1}{2} \tag{A-16}$$

To insure that $\mu > 0$, equation A-14 must be:

$$\mu = \frac{4\eta - 1}{1 - 2\eta + \sqrt{-12\eta^2 + 12\eta - 2}} \tag{A-17}$$

Moments of Inertia of a Frustum of a Right Circular Cone

The moment of inertia about the X-axis of the element of mass shown in figure 12 is given by:

$$I_x = \int_o^{\ell} dI'_x + \int_o^{\ell} Y^2 dm \tag{A-18}$$

where dI'_x is the moment of inertia of the element about the X'-axis (see figure 12) and dm is given by equation A-2. Since the element of mass is a thin circular disc, its moment of inertia about an axis through its center of mass is given by:

$$dI'_x = \frac{r^2 dm}{4} = \frac{\delta \pi}{4} X^4 dY \tag{A-19}$$

Substituting equations A-2 and A-19 into A-18 and carrying out the integration:

$$I_x = \delta\pi \int_o^{\ell} \left(\frac{X^4}{4} + X^2 Y^2\right) dY \tag{A-20}$$

$$= \frac{\delta \pi \ell}{20}(R^4 + R^3 r + R^2 r^2 + R r^3 + r^4)$$

$$+ \frac{\delta \pi \ell^3}{30}(R^2 + 3Rr + 6r^2) \tag{A-21}$$

After some rearranging, we get:

$$I_x = \frac{\delta \pi \ell \sigma R^2}{3}\left[\frac{3R^2}{20\sigma}(1 + \mu + \mu^2 + \mu^3 + \mu^4)\right.$$

$$\left. + \frac{\ell^2}{10\sigma}(1 + 3\mu + 6\mu^2)\right] \tag{A-22}$$

where:

$$\sigma = 1 + \mu + \mu^2 \tag{A-23}$$

Equation A-5 can be written:

$$m = \frac{\delta \pi \ell \sigma R^2}{3} \tag{A-24}$$

or:

$$R^2 = \frac{3m}{\delta \pi \ell \sigma} \tag{A-25}$$

Substituting equations A-24 and A-25 into A-22:

$$I_x = m\left\{\frac{9}{20\pi}\left(\frac{1 + \mu + \mu^2 + \mu^3 + \mu^4}{\sigma^2}\right)\left(\frac{m}{\delta \ell}\right)\right.$$

$$\left. + \frac{1}{10}\left(\frac{1 + 3\mu + 6\mu^2}{\sigma}\right)\ell^2\right\} \tag{A-26}$$

Letting:

$$A = \frac{9}{20\pi}\left(\frac{1 + \mu + \mu^2 + \mu^3 + \mu^4}{\sigma^2}\right) \tag{A-27}$$

and:

$$C = \frac{1}{10}\left(\frac{1 + 3\mu + 6\mu^2}{\sigma}\right) \tag{A-28}$$

then:

$$I_x = m\left[A\left(\frac{m}{\delta \ell}\right) + C\,\ell^2\right] \tag{A-29}$$

By the Parallel Axis Transfer Theorem:

$$I_x = I_{x_{CG}} + mD^2 \tag{A-30}$$

then:

$$I_{x_{CG}} = I_x - mD^2 \tag{A-31}$$

Substituting equations A-10 and A-29 into the above equation:

$$I_{x_{CG}} = m\left[\frac{9}{20\pi}\left(\frac{1 + \mu + \mu^2 + \mu^3 + \mu^4}{\sigma^2}\right)\frac{m}{\delta \ell} + \frac{3}{80}\left(\frac{1 + 4\mu + 10\mu^2 + 4\mu^3 + \mu^4}{\sigma^2}\right)\ell^2\right] \tag{A-32}$$

$$I_{x_{CG}} = m\left[A\left(\frac{m}{\delta \ell}\right) + B\,\ell^2\right] \tag{A-33}$$

where:

$$B = \frac{3}{80}\left(\frac{1 + 4\mu + 10\mu^2 + 4\mu^3 + \mu^4}{\sigma^2}\right) \tag{A-34}$$

Now:

$$I_y = \int_0^{\ell} dI_y' \tag{A-35}$$

where:

$$dI_y' = \tfrac{1}{2}\, r^2\, dm \tag{A-36}$$

$$= \tfrac{1}{2}\,\delta\pi\, X^4\, dY \tag{A-37}$$

By an approach similar to that above, we get:

$$I_y = \frac{2m^2}{\delta \ell}\, A \tag{A-38}$$

Since the frustum is a body of revolution, then:

$$I_x = I_z \tag{A-39}$$

In equations A-29, A-33, and A-38 the quantities A, B, and C are constant for a given value of η. With the AFIT IBM 1620 Digital Computer and the assistance of Prof. R. T. Harling of the Department of Mathematics, the values of μ, A, B, and C were calculated for intervals of 0.001 over the range $0.250 \leq \eta \leq 0.500$. The results are presented graphically in figure 13.

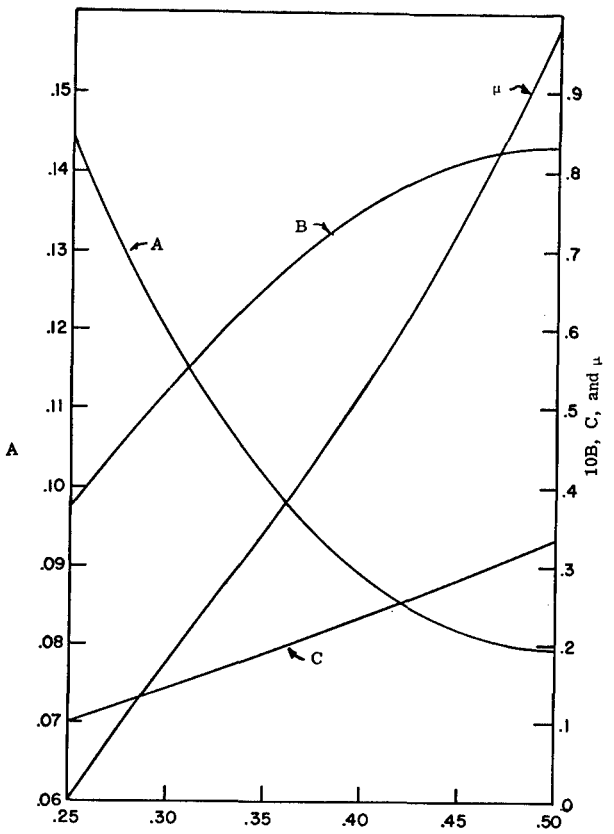

Figure 13. Parameters A, B, C, and μ versus η

The following Fortran Computer Program was used, where R ≡ η, U ≡ μ, S ≡ σ, and H is the interval between successive values of R.

```
      ACCEPT, H, RIN
      R = RIN
      PI = 3.14159265
4     U = (4.*R-1.)/(1.-2.*R+(-12.*R*R+12.*R-2.)**0.5)
      U2 = U*U
      U3 = U2*U
      U4 = U3*U
      S = 1.+U+U2
      A = ((S+U3+U4)*9.)/(20.*PI*S*S)
      B = ((1.+4.*U+10.*U2+4.*U3+U4)*3.)/(80.*S*S)
      C = ((1.+3.*U+6.*U2)*0.1)/S
      IF (SENSE SWITCH 2 ) 13, 14
13    PRINT 19,R,U,S,A,B,C
14    PUNCH 21,R,U,S,A,B,C
      R = R + H
      IF (R-0.501) 4,18,18
18    STOP
19    FORMAT (/F 5.3,F10.5,F11.5,3F10.5)
21    FORMAT (F5.3,F10.5,F11.5,3F10.5)
      END
```

Note that when $\eta = 0.250$ the frustum reduces to a right circular cone, and when $\eta = 0.500$ the frustum becomes a right circular cylinder.

This is reflected by the equations for moments of inertia. For example, when $\eta = 0.250$, $\mu = 0$, and $\sigma = 1$, equations A-27, A-28, and A-34 yield:

$$A = 0.14323 \qquad B = 0.03750 \qquad C = 0.10000$$

Then equations A-33 and A-39 become:

$$I_{x_{CG}} = I_{z_{CG}} = m\left[0.14323\left(\frac{m}{\delta \ell}\right) + 0.03750\ \ell^2\right]$$

and equation A-38 becomes:

$$I_{y_{CG}} = \frac{2m^2}{\delta \ell}\ (0.14323)$$

Now the mass of a right circular cone is given by:

$$m = \frac{\pi \delta \ell}{3}\ r^2 = 1.0478\ \delta\ \ell^2$$

so that:

$$I_{x_{CG}} = I_{z_{CG}} = m\left[0.14323\left(\frac{1.0478\ \delta\ \ell\ r^2}{\delta\ \ell}\right) + 0.03750\ \ell^2\right]$$

$$= m\,(0.1500\ r^2 + 0.0375\ \ell^2)$$

$$= \frac{3}{20}\ m\left(r^2 + \frac{\ell^2}{4}\right)$$

and:

$$I_{y_{CG}} = m\left[0.14323\left(\frac{2 \times 1.0478\ \delta\ \ell\ r^2}{\delta\ \ell}\right)\right]$$

$$= 0.3000\ mr^2$$

$$= \frac{3}{10}\ mr^2$$

These are the exact equations for moments of inertia of a right circular cone.

Similarly, when $\eta = 0.500$, $\mu = 1$, $\sigma = 3$, then:

$$A = 0.07957 \qquad B = 0.08333 \qquad C = 0.3333$$

and:

$$I_{x_{CG}} = I_{z_{CG}} = m\left[0.07957\left(\frac{m}{\delta \ell}\right) + 0.08333\ \ell^2\right]$$

$$I_{y_{CG}} = \frac{2m^2}{\delta \ell}\ (0.07957)$$

Now the mass of a right circular cylinder is given by:

$$m = \delta\ \pi\ r^2\ \ell$$

so that:

$$I_{x_{CG}} = I_{z_{CG}} = m\left[0.07957\left(\frac{\delta \ell \pi r^2}{\delta \ell}\right) + 0.08333\ \ell^2\right]$$

$$= m\ [0.2500\ r^2 + 0.08333\ \ell^2\ ]$$

$$= \frac{m}{12}\left[3r^2 + \ell^2\right]$$

and:

$$I_{y_{CG}} = m(0.07957)\left(\frac{2 \times \delta \pi r^2 \ell}{\delta \ell}\right)$$

$$= 0.5000\ mr^2$$

$$= \frac{mr^2}{2}$$

These are the exact equations for moments of inertia of a right circular cylinder.

Sample Calculation

Find the local moments of inertia of the upper arm of the Air Force mean man.

From table V:

$$\eta = 0.436$$

From equations A-14, A-27, A-34, and A-28, or figure 13:

$\mu = 0.67445$ A = 0.08349
B = 0.08006 C = 0.27016

Equations A-29, A-33, and A-38 become:

$$I_x = I_z = m\left[0.08349\left(\frac{m}{\delta \ell}\right) + 0.2716\ \ell^2\right]$$

$$I_{x_{CG}} = I_{z_{CG}} = m\left[0.08349\left(\frac{m}{\delta \ell}\right) + 0.08006\ \ell^2\right]$$

$$I_y = I_{y_{CG}} = 0.16698\frac{m^2}{\delta \ell}$$

Also, from table V:

$\delta = 70.0$ lbs/ft^3
$\ell = 13.0$ in.
$m = 5.10$ lbs

then the moments of inertia about the mass center are found to be:

$$I_{x_{CG}} = I_{z_{CG}} = \frac{5.10}{32.2}\left[\frac{0.08349 \times 5.10}{70.0 \times \frac{13.0}{12.0}} + 0.08006\left(\frac{13.0}{12.0}\right)^2\right]$$

$$= 0.0157\ \text{slug-ft}^2$$

$$I_{y_{CG}} = \frac{0.16698\left(\frac{5.10}{32.2}\right)^2}{\left(\frac{70.0}{32.2}\right)\left(\frac{13.0}{12.0}\right)}$$

$$= 0.00178\ \text{slug-ft}^2$$

APPENDIX B

EQUATIONS OF MOTION FOR THE THRUST MISALIGNMENT PROBLEM

Symbols

X, Y, Z Body axis system coordinates (coinciding with the principal axes)
X′, Y′, Z′ Fixed or inertial axis system
$\hat{i}$, $\hat{j}$, $\hat{k}$ Unit vectors corresponding to the body axis system
$\hat{i}'$, $\hat{j}'$, $\hat{k}'$ Unit vectors corresponding to the inertial axis system
I_x, I_y, I_z Principal mass moments of inertia

Conditions

The following conditions are assumed for solution of the equations of motion for the thrust misalignment problem:

a. Rigid body
b. Constant mass, m
c. Constant moment about the body Y-axis
d. Constant thrust, F, in the direction of the body X-axis
e. $I_x = I_y$

Using a vector notation:

Force vector $\hat{F} = F\hat{i}$ (B-1)

Position vector $\hat{\epsilon} = \epsilon\hat{k}$ (B-2)

Moment vector $\hat{M} = \hat{\epsilon} \times \hat{F}$ (B-3)

$= \epsilon\hat{k} \times F\hat{i} = \epsilon F\hat{j}$ (B-4)

But:

$\hat{M} = M_x\hat{i} + M_y\hat{j} + M_z\hat{k}$ (B-5)

Therefore:

$M_x = M_z = 0$ (B-6)

and:

$M_y = \epsilon F$ (B-7)

Then Euler's Equations:

$$M_x = I_x \dot{\omega}_x + (I_z - I_y)\ \omega_y\ \omega_z \tag{B-8}$$

$$M_y = I_y \dot{\omega}_y + (I_x - I_z)\ \omega_x\ \omega_z \tag{B-9}$$

$$M_z = I_z \dot{\omega}_z + (I_y - I_x)\ \omega_x\ \omega_y \tag{B-10}$$

become:

$$0 = I_x \dot{\omega}_x + (I_z - I_x)\ \omega_y\ \omega_z \tag{B-11}$$

$$\epsilon F = I_y \dot{\omega}_y + (I_x - I_z)\ \omega_x\ \omega_z \tag{B-12}$$

$$0 = I_z \dot{\omega}_z \tag{B-13}$$

From equation B-13:

$$I_z\ \omega_z = \text{constant} \tag{B-14}$$

If the body is initially at rest:

$$\omega_z = 0 \tag{B-15}$$

and the constant is zero. Equations B-11 and B-12 become:

$$0 = I_x \dot{\omega}_x \tag{B-16}$$

$$\epsilon F = I_y \dot{\omega}_y \tag{B-17}$$

By the same reasoning applied to equation B-13, equation B-16 yields:

$$\omega_x = 0 \tag{B-18}$$

Also equation B-17 yields:

$$\omega_y = \frac{\epsilon F}{I_y}\ t \tag{B-19}$$

for zero initial conditions.

Now:

$$\hat{\omega} = \omega_x \hat{i} + \omega_y \hat{j} + \omega_z \hat{k} \tag{B-20}$$

but by equations B-15, B-18, and B-19:

$$\hat{\omega} = \omega_y \hat{j} = \frac{\epsilon F}{I_y}\ t\hat{j} \tag{B-21}$$

When the products of inertia are zero, angular momentum about the mass center of a rotating body is given by:

$$\hat{H}_c = I_x \omega_x \hat{i} + I_y \omega_y \hat{j} + I_z \omega_z \hat{k} \tag{B-22}$$

Substituting equations B-15 and B-18 into equation B-22:

$$\hat{H}_c = I_y \omega_y \hat{j} = h_y \hat{j} \tag{B-23}$$

Hence:

$$h_x = h_z = 0 \tag{B-24}$$

Now the moment about the mass center is given by:

$$\hat{M}_c = \dot{\hat{H}}_c + \hat{\omega} \times \hat{H}_c \tag{B-25}$$

After substituting and carrying out the indicated operations:

$$\epsilon F \hat{j} = \dot{h}_Y \hat{j} + \omega_Y \hat{j} \times h_Y \hat{j} \tag{B-26}$$

$$= \dot{h}_Y \hat{j} \tag{B-27}$$

Therefore, this moment increases the magnitude of the angular momentum, but does not change its direction. Hence, the angular momentum and angular velocity vectors remain parallel and fixed (in direction) in space. The only rotation is, then, a spin about the body Y-axis which also remains fixed (in direction) in space. The thrust is then applied in a plane perpendicular to the Y-axis and the resulting translation is in the same plane. If the body axis system is initially aligned with the inertial axis system, then the body XZ-plane will remain in the inertial XZ-plane. The only motion between the two axis systems is translation in the inertial XZ-plane and rotation about the body Y-axis. The unit vector transformation becomes:

$$\hat{i} = \hat{i}' \cos\beta - k \sin\beta \tag{B-28}$$

$$\hat{j} = \hat{j}' \tag{B-29}$$

where β is the angle between the Z- and Z'-axes (or rotation between the two axis systems).

By Newton's Equation:

$$\hat{F} = m\hat{a}' \tag{B-30}$$

$$F\hat{i} = m(a_{X'}\hat{i}' + a_{Y'}\hat{j}' + a_{Z'}\hat{k}') \tag{B-31}$$

but:

$$F\hat{i} = \hat{i}' F\cos\beta - \hat{j}' F\sin\beta \tag{B-32}$$

or:

$$\hat{i}' F\cos\beta - \hat{j}' F\sin\beta = m a_{X'}\hat{i}' + m a_{Y'}\hat{j}' + m a_{Z'}\hat{k}' \tag{B-33}$$

therefore:

$$F\cos\beta = m a_{X'} \tag{B-34}$$

$$0 = m a_{Y'} \tag{B-35}$$

$$-F\sin\beta = m a_{Z'} \tag{B-36}$$

and:

$$\ddot{X}' = \frac{F}{m}\cos\beta \tag{B-37}$$

$$\ddot{Y}' = 0 \tag{B-38}$$

$$\ddot{Z}' = -\frac{F}{m}\sin\beta \tag{B-39}$$

Now the angular velocity of the body-fixed axis system with respect to the inertial system is:

$$\hat{\omega} = \dot{\beta}\hat{j}' \tag{B-40}$$

and from equation B-21:

$$\frac{\epsilon F t \hat{j}}{I_Y} = \dot{\beta}\hat{j}' = \dot{\beta}\hat{j} \tag{B-41}$$

Therefore:

$$\dot{\beta} = \frac{\epsilon F t}{I_Y} \tag{B-42}$$

and integrating:

$$\beta = \frac{\epsilon F t^2}{2 I_Y} = K t^2 \tag{B-43}$$

for $\dot{\beta} = 0$ at $t = 0$, and:

$$K = \frac{\epsilon F}{2I_y} \tag{B-44}$$

Substituting for β in equations B-37 and B-39 and integrating, the coordinates of the trajectory become:

$$X' = \frac{F}{m} \iint \cos Kt^2 \, dt \, dt \tag{B-45}$$

$$Y' = 0 \tag{B-46}$$

$$Z' = -\frac{F}{m} \iint \sin Kt^2 \, dt \, dt \tag{B-47}$$

Equations B-45 and B-47 can be nondimensionalized by substituting:

$$\tau^2 = Kt^2 \tag{B-48}$$

$$X_n' = \frac{mK}{F} X' \tag{B-49}$$

$$Z_n' = \frac{mK}{F} Z' \tag{B-50}$$

Then:

$$X_n' = \iint \cos \tau^2 \, d\tau \, d\tau \tag{B-51}$$

$$Z_n' = -\iint \sin \tau^2 \, d\tau \, d\tau \tag{B-52}$$

Note also:

$$dX_n'/d\tau = \dot{X}_n' = \int \cos \tau^2 \, d\tau \tag{B-53}$$

$$dZ_n'/d\tau = \dot{Z}_n' = -\int \sin \tau^2 \, d\tau \tag{B-54}$$

Solution

Equations B-51, B-52, B-53, and B-54 could not be integrated to get a closed form solution. However, a numerical solution was achieved by applying the Runge-Kutta Method (ref. 16) and computing the functions point by point on the AFIT IBM 1620 Digital Computer. The following Fortran input program was used where:

$T \equiv \tau$
$X \equiv X_n'$
$Z \equiv Z_n'$
$H \equiv$ Interval between points
$XP \equiv dX_n'/d\tau$
$ZP \equiv dZ_n'/d\tau$

and the "IN" after the above symbols refers to initial conditions. The results are given graphically in figures 14 and 15.

```
ACCEPT, H, TIN, XIN, XPIN, ZIN, ZPIN
T = TIN
X = XIN
Z = ZIN
XP = XPIN
ZP = ZPIN
1 PRINT, T, X, XP, Z, ZP
F1 = H * CØS(T*T)
F2 = H * CØS((T + .5 * H)** 2)
F3 = F2
F4 = H * CØS((T + H)** 2)
DELX = H * (XP + (F1 + F2 + F3)/6.)
DELXP = (F1 + 2.*(F2 + F3) + F4)/6.
X = X + DELX
XP = XP + DELXP
F1 = - H * SIN(T*T)
F2 = -H * SIN((T + .5*H)**2)
F3 = F2
F4 = -H * SIN((T + H)**2)
DELZ = H * (ZP + (F1 + F2 + F3)/6.)
DELZP = (F1 + 2.*(F2 + F3) + F4)/6.
Z = Z + DELZ
ZP = ZP + DELZP
T = T + H
GØ TØ 1
END
```

The solution is then:

$$X = NX' \tag{B-55}$$
$$Z = NZ' \tag{B-56}$$
$$\dot{X} = N\sqrt{k}\,\dot{X}' \tag{B-57}$$
$$\dot{Z} = N\sqrt{k}\,\dot{Z}' \tag{B-58}$$
$$\beta = kt^2 \tag{B-59}$$
$$\dot{\beta} = 2kt \tag{B-60}$$

where:

$$N = \frac{2I_y}{\epsilon m} \tag{B-61}$$

Example

The USAF mean man is equipped with a thrust device rigidly attached to his back so that its thrust vector passes through his center of mass when he is in position A (figure 5). However, just before firing the device (capable of generating 10 pounds of thrust), he changes to position B. What is the resulting motion, assuming the conditions previously listed apply?

From equation 24 and the tabular data in tables V, VI, and VII:

$$\overline{Z} = \frac{\sum_{i=1}^{n} m_i(Z_i - Z_{i_o})}{m_{tot}}$$

$$= \{2[1.16(14.672 + 7.406)] + 2[3.03(8.138 - 0.114)]$$

$$+ 2[16.33(1.355 + 11.406)] + 2[8.05(2.181 + 27.286)]$$

$$+ 2[2.39(-8.256 + 37.716)]\} \div 162.22 = 6.977 \text{ in.} = \epsilon$$

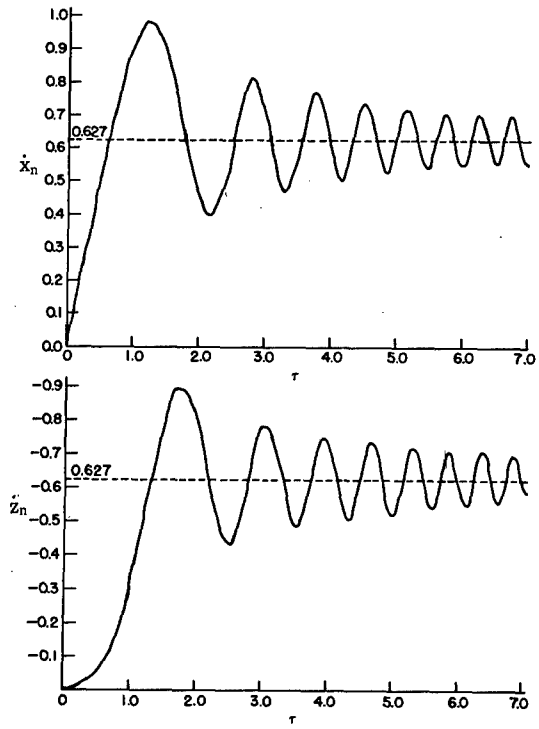

Figure 14. Nondimensional Velocity Components As a Function of τ

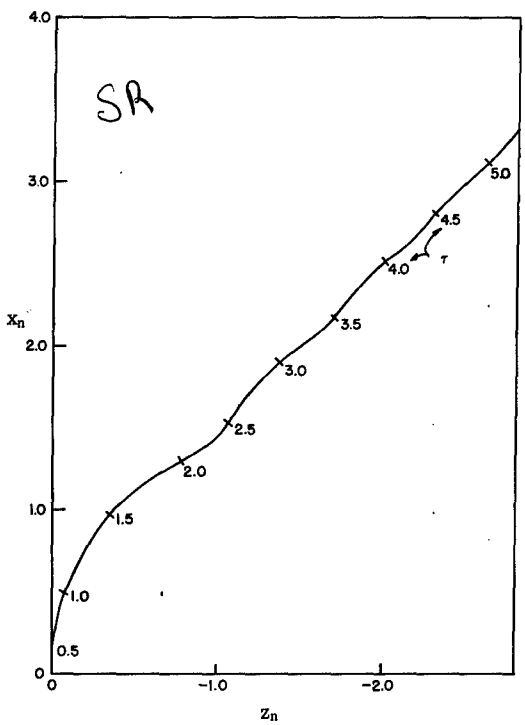

Figure 15. Nondimensional Trajectory As a Function of τ

For the USAF mean man:

$$m = 5.0379 \text{ slugs}$$
$$I_Y = 2.9445 \text{ slug-ft}^2$$

Then equation B-44 yields:

$$K = \frac{\frac{6.977}{12} \times 10}{2 \times 2.9445} = 0.9873/\text{sec}^2$$

and from equation B-61:

$$N = \frac{2 \times 2.9445}{\frac{6.977}{12} \times 5.0379} = 2.0105/\text{ft}$$

Equation B-48 yields:

$$\tau = 0.994t$$

and equations B-55 through B-60 become:

$$X = 2.01X' \qquad \dot{X} = 2.00\dot{X}'$$
$$Z = 2.01A' \qquad \dot{Z} = 2.00\dot{Z}'$$
$$\beta = 0.987t^2 \qquad \dot{\beta} = 1.975t$$

The values of these functions are given for various times in table X.

TABLE X

NUMERICAL RESULTS OF THE MISALIGNED THRUST PROBLEM

t (seconds)	X (feet)	$\dot{X}$ (ft/sec)	Z (feet)	$\dot{Z}$ (ft/sec)	β (degrees)	$\dot{\beta}$ (rpm)
1.008	0.160	1.900	-0.162	-0.649	57.5	19.2
2.016	2.620	0.924	-1.572	-1.610	230.0	38.3
3.022	3.830	1.411	-2.740	-1.553	516.0	57.5
5.030	6.280	1.223	-5.300	-1.056	1430.9	95.9
10.060	12.590	1.202	-11.590	-1.167	5720.0	191.4

APPENDIX C

FREE-BODY DYNAMICS PROBLEM

Symbols

$\hat{e}_1$, $\hat{e}_2$, $\hat{e}_3$	Unit vectors corresponding to the X, Y, Z Body-Fixed Axis System at the mass center of mass, m_2
$\hat{E}_1$, $\hat{E}_2$, $\hat{E}_3$	Unit vectors corresponding to the X′, Y′, Z′ Body-Fixed Axis System at the mass center of mass, m_1
$\hat{Q}_1$, $\hat{Q}_2$	Position vectors from the hinge point to the individual mass centers
$\hat{\omega}$	Angular velocity of mass, m_2
$\hat{\Omega}$	Angular velocity of mass, m_1
$\hat{\lambda}$	Net angular velocity of the system
$\hat{H}_c$	Total angular momentum of the system about the mass center
$\hat{h}_1$	Angular momentum of mass, m_1
$\hat{h}_2$	Angular momentum of mass, m_2
I_1	Moment of inertia of mass, m_1, about its mass center
I_2	Moment of inertia of mass, m_2, about its mass center

Deviation of Equations

The system of two rigid masses shown in figure 16 is hinged at point G so that the mass centers and point G remain in the same plane. Assume that initially:

$$\gamma = 0 \tag{C-1}$$
$$\dot{\gamma} = \text{constant} = \lambda \tag{C-2}$$
$$\hat{H}_c = 0 \tag{C-3}$$

and there are no external forces. From figure 16 it can be seen that:

$$\hat{Q}_1 = Q_1 \hat{E}_1 \tag{C-4}$$
$$\hat{Q}_2 = -Q_2 \hat{e}_1 = -Q_2 \cos\gamma \hat{E}_1 - Q_2 \sin\gamma \hat{E}_2 \tag{C-5}$$
$$\hat{\omega} = \omega \hat{e}_3 = \omega \hat{E}_3 \tag{C-6}$$
$$\hat{\Omega} = -\Omega \hat{E}_3 \tag{C-7}$$
$$\dot{\gamma} \hat{e}_3 = \hat{\lambda} = \lambda \hat{E}_3 \tag{C-8}$$
$$\hat{h}_1 = -I_1 \Omega \hat{E}_3 \tag{C-9}$$
$$\hat{h}_2 = I_2 \omega \hat{e}_3 = I_2 (\lambda - \Omega) \hat{e}_3 \tag{C-10}$$

Since c.c.m. is the mass center of the whole system:

$$m_1 D_1 + m_2 D_2 = 0 \tag{C-11}$$

or:

$$\hat{D}_2 = -\frac{m_1}{m_2} \hat{D}_1 = -\frac{1}{\Psi} \hat{D}_1 \tag{C-12}$$

where Ψ is the mass ratio, $\frac{m_2}{m_1}$.

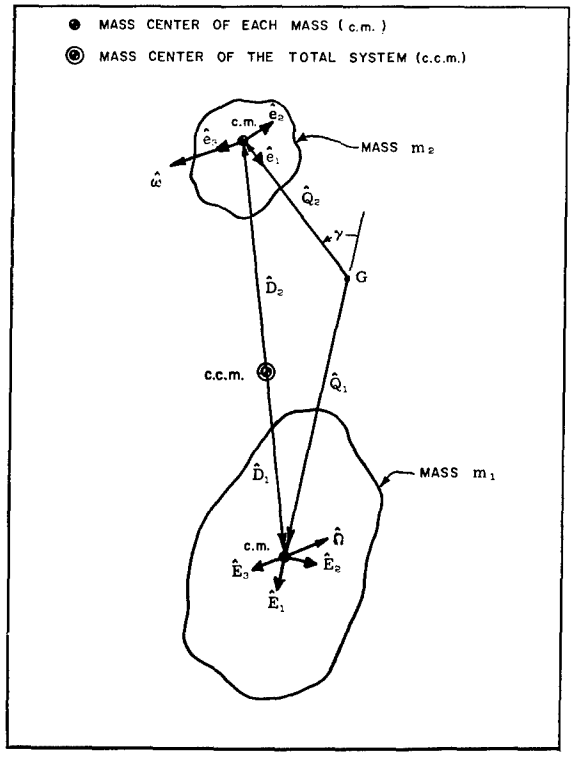

Figure 16. Vector Diagram and Body-Fixed Axis Systems

Now define:

$$\hat{D}_1 + \hat{\Delta} = \hat{D}_2 \tag{C-13}$$

Solving equations C-12 and C-13 simultaneously:

$$\dot{\hat{D}}_1 = -\hat{\Delta}(1 + \Psi)^{-1}\,\Psi \tag{C-14}$$

$$\hat{D}_2 = \hat{\Delta}\,(1 + \Psi)^{-1} \tag{C-15}$$

The total momentum of the system can be written (ref. 10):

$$\hat{H}_c = \hat{h}_1 + m_1\hat{D}_1 \times \dot{\hat{D}}_1 + \hat{h}_2 + m_2\hat{D}_2 \times \dot{\hat{D}}_2 \tag{C-16}$$

and by equation C-3:

$$0 = \hat{h}_1 + m_1\hat{D}_1 \times \dot{\hat{D}}_1 + \hat{h}_2 + m_2\hat{D}_2 \times \dot{\hat{D}}_2 \tag{C-17}$$

Substituting equations C-9, C-10, C-14, and C-15 into equation C-17, then:

$$-I_1\,\Omega\,\hat{E}_3 + m_1[\hat{\Delta}\,(1 + \Psi)^{-1}\Psi] \times [\dot{\hat{\Delta}}(1 + \Psi)^{-1}\,\Psi] + I_2(\lambda - \Omega)\,\hat{E}_3$$

$$+ m_2[\hat{\Delta}\,(1 + \Psi)^{-1}] \times [\dot{\hat{\Delta}}\,(1 + \Psi)^{-1}] = 0 \tag{C-18}$$

where:

$$\dot{\hat{D}}_1 = -\dot{\hat{\Delta}}(1+\Psi)^{-1}\Psi \tag{C-19}$$

$$\dot{\hat{D}}_2 = \dot{\hat{\Delta}}(1+\Psi) \tag{C-20}$$

Now:

$$\hat{\Delta} = \hat{D}_2 - \hat{D}_1 \tag{C-21}$$

$$= -(Q_1 + Q_2\cos\gamma)\,\hat{E}_1 + (-Q_1\sin\gamma)\,\hat{E}_2 \tag{C-22}$$

and:

$$\dot{\hat{\Delta}} = \hat{\Delta}' + \hat{\Omega} \times \hat{\Delta} \tag{C-23}$$

Equation C-23 becomes after simplification:

$$\dot{\hat{\Delta}} = (\lambda - \Omega)\,Q_2\sin\gamma\,\hat{E}_1 + [Q_1\Omega + Q_2(\Omega-\lambda)\cos\gamma]\,\hat{E}_2 \tag{C-24}$$

Substituting equation C-24 into C-18 and carrying out the indicated operations, equation C-18 becomes:

$$[(I_1 + I_2)\Omega - I_2\lambda]\,\hat{E}_3 = (m_1\Psi^2 + m_2)(1+\Psi)^{-2}$$

$$[-(Q_1^2 + Q_2^2 + 2Q_1Q_2\cos\gamma)\Omega + (Q_2^2 + Q_1Q_2\cos\gamma)\lambda]\,\hat{E}_3 \tag{C-25}$$

Equating the scalar components and combining, equation C-25 reduces to:

$$[I_1 + I_2 + (Q_1^2 + Q_2^2 + 2Q_1Q_2\cos\gamma)\,m_2\,(1+\Psi)^{-1}]\,\Omega$$

$$= [I_2 + Q_2(Q_2 + Q_1\cos\gamma)\,m_2(1+\Psi)^{-1}]\lambda \tag{C-26}$$

or:

$$I_1(t)\,\Omega(t) = I_2(t)\,\lambda \tag{C-27}$$

where $I_1(t)$ and $I_2(t)$ are instantaneous moments of inertia and:

$$I_1(t) = I_1 + I_2 + (Q_1^2 + Q_2^2 + 2Q_1Q_2\cos\gamma)m_2(1+\Psi)^{-1} \tag{C-28}$$

$$I_2(t) = I_2 + Q_2(Q_2 + Q_1\cos\gamma)\,m_2(1+\Psi)^{-1} \tag{C-29}$$

Let:

$$\Omega(t) = \frac{d\nu}{dt} = \dot{\nu} \tag{C-30}$$

then:

$$d\nu = \frac{I_2(t)}{I_1(t)}\,\lambda\,dt \tag{C-31}$$

Now:

$$\gamma = \lambda t \tag{C-32}$$

or:

$$d\gamma = \lambda\,dt \tag{C-33}$$

Substituting equation C-33 in equation C-31 and integrating:

$$\int_0^{\nu} d\nu = \int_0^{\gamma} \frac{I_1(t)}{I_2(t)}\,d\gamma \tag{C-34}$$

Equations C-28 and C-29 can be written:

$$I_1(t) = C + D\cos\gamma \tag{C-35}$$

$$I_2(t) = A + B\cos\gamma \tag{C-36}$$

where:

$$A = I_2 + Q_2^2\, m_2(1 + \Psi)^{-1} \tag{C-37}$$

$$B = Q_1 Q_2\, m_2(1 + \Psi)^{-1} \tag{C-38}$$

$$C = I_1 + I_2 + (Q_1^2 + Q_2^2)\, m_2(1 + \Psi)^{-1} \tag{C-39}$$

$$D = 2Q_1 Q_2\, m_2(1 + \Psi)^{-1} \tag{C-40}$$

and are constant for a given problem. Equation C-34 then becomes:

$$\nu = \int_0^{\gamma} \frac{A + B\cos\gamma}{C + D\cos\gamma}\, d\gamma \tag{C-41}$$

Integrating the right side of equation C-41:

$$\nu = \frac{\gamma}{2} + \frac{(2A - C)}{\sqrt{C^2 - D^2}} \arctan\left(\frac{\sqrt{C^2 - D^2}}{C + D} \tan\frac{\gamma}{2}\right) \tag{C-42}$$

$$\nu = \frac{\gamma}{2} + \frac{I_4}{I_3} \arctan\left(\frac{I_3 \tan\frac{\gamma}{2}}{I_1(0)}\right) \tag{C-43}$$

where:

$$I_3 = \sqrt{C^2 - D^2} = [(I_1 + I_2)^2 + 2m_2(I_1 + I_2)(Q_1^2 + Q_2^2)(1 + \Psi)^{-1} + m_2^2(Q_1^2 - Q_2^2)^2(1 + \Psi)^{-2}]^{\frac{1}{2}} \tag{C-44}$$

$$I_4 = 2A - C = I_2 - I_1 + m_2(1 + \Psi)^{-1}(Q_2^2 - Q_1^2) \tag{C-45}$$

$$I_1(0) = C + D = I_1(t)\big|_{\text{at } t = 0} \tag{C-46}$$

$$= I_2 + I_1 + (Q_1^2 + Q_2^2)\, m_2(1 + \Psi)^{-1} + 2Q_1 Q_2 m_2(1 + \Psi)^{-1} \tag{C-47}$$

Hence, the change in the attitude of the large mass, m_1, is a function of the rotation, γ, of the small mass, m_2.

Example

If the small mass, m_2, represents both arms (including the hands) of the USAF mean man, and m_1 represents the total mass less that of m_2, equation C-43 can be used to calculate the change in body attitude when the arms are rotated. Then, from the tabular data in tables V, VI, and VII, and the above equations:

$Q_1 = 1.511$ ft $I_1 = 8.6811$ slug-ft^2
$Q_2 = 0.988$ ft $I_3 = 10.4866$ slug-ft^2
$\Psi = 0.1294$ $I_4 = -9.0980$ slug-ft^2
$I_2 = 0.2508$ slug-ft^2 $I_1(0) = 12.1223$ slug-ft^2

and:

$$\nu = \frac{\gamma}{2} - 0.8676 \arctan\left(0.86507 \tan\frac{\gamma}{2}\right)$$

for $\gamma = 360°$:

$$\nu = 180° - 0.8676\,(180°)$$
$$= 23.84°$$